

ITIC FILE COPY

4

GL-TR-89-0261

Three Recent Larger Earthquakes Offshore Norway

Roger A. Hansen
Hilmar Bungum
Alfred Alsaker

NTNF/NORSAR
P.O. Box 51
N-2007 Kjeller, NORWAY

31 August 1989

Scientific Report No. 2

APPROVED FOR PUBLIC RELEASE; DISTRIBUTION UNLIMITED

GEOPHYSICS LABORATORY
AIR FORCE SYSTEMS COMMAND
UNITED STATES AIR FORCE
HANSCOM AIR FORCE BASE, MASSACHUSETTS 01731-5000

DTIC
ELECTE
JAN 02 1990
S B D

90 01 02 056

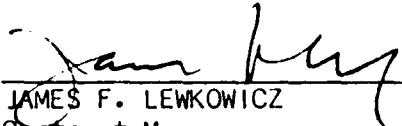
AD-A216 261

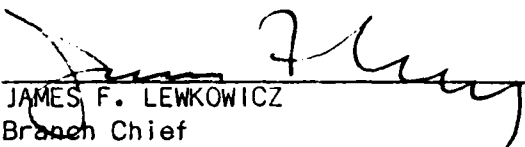
SPONSORED BY
Defense Advanced Research Projects Agency
Nuclear Monitoring Research Office
ARPA ORDER NO. 5307

MONITORED BY
Geophysics Laboratory
Contract No. F49620-89-C-0038


The views and conclusions contained in this document are those of the authors and should not be interpreted as representing the official policies, either expressed or implied, of the Defense Advanced Research Projects Agency or the U.S. Government.

This technical report has been reviewed and is approved for publication.


JAMES F. LEWKOWICZ
Contract Manager
Solid Earth Geophysics Branch
Earth Sciences Division


JAMES F. LEWKOWICZ
Branch Chief
Solid Earth Geophysics Branch
Earth Sciences Division

FOR THE COMMANDER


DONALD H. ECKHARDT, Director
Earth Sciences Division

This report has been reviewed by the ESD Public Affairs Office (PA) and is releasable to the National Technical Information Service (NTIS).

Qualified requestors may obtain additional copies from the Defense Technical Information Center. All others should apply to the National Technical Information Service.

If your address has changed, or if you wish to be removed from the mailing list, or if the addressee is no longer employed by your organization, please notify GL/IMA, Hanscom AFB, MA 01731-5000. This will assist us in maintaining a current mailing list.

Do not return copies of this report unless contractual obligations or notices on a specific document requires that it be returned.

Unclassified

SECURITY CLASSIFICATION OF THIS PAGE

REPORT DOCUMENTATION PAGE				Form Approved OMB No. 0704-0188	
1a. REPORT SECURITY CLASSIFICATION Unclassified			1b. RESTRICTIVE MARKINGS		
2a. SECURITY CLASSIFICATION AUTHORITY			3. DISTRIBUTION/AVAILABILITY OF REPORT Approved for public release; Distribution unlimited		
2b. DECLASSIFICATION/DOWNGRADING SCHEDULE					
4. PERFORMING ORGANIZATION REPORT NUMBER(S)			5. MONITORING ORGANIZATION REPORT NUMBER(S) GL-TR-89-0261		
6a. NAME OF PERFORMING ORGANIZATION NTNF/NORSAR		6b. OFFICE SYMBOL (If applicable)	7a. NAME OF MONITORING ORGANIZATION Geophysics Laboratory		
6c. ADDRESS (City, State, and ZIP Code) Post Box 51 N-2007 Kjeller, Norway			7b. ADDRESS (City, State, and ZIP Code) Hanscom Air Force Base Massachusetts 01731-5000		
8a. NAME OF FUNDING/SPONSORING ORGANIZATION Defence Advanced Research Projects Agency		8b. OFFICE SYMBOL (If applicable) NMRO	9. PROCUREMENT INSTRUMENT IDENTIFICATION NUMBER Contract No. F49620-89-C-0038		
8c. ADDRESS (City, State, and ZIP Code) 1400 Wilson Blvd. Arlington, VA 22209-2308			10. SOURCE OF FUNDING NUMBERS		
			PROGRAM ELEMENT NO. 62714E	PROJECT NO. 9A10	TASK NO. DA
					WORK UNIT ACCESSION NO. BH
11. TITLE (Include Security Classification) Three recent larger earthquakes offshore Norway					
12. PERSONAL AUTHOR(S) Roger A. Hansen, Hilmar Bungum and Alfred Alsaker					
13a. TYPE OF REPORT SCIENTIFIC REP. 2		13b. TIME COVERED FROM 89/05/01 TO 89/07/31		14. DATE OF REPORT (Year, Month, Day) 1989 August 31	
				15. PAGE COUNT 54	
16. SUPPLEMENTARY NOTATION					
17. COSATI CODES			18. SUBJECT TERMS (Continue on reverse if necessary and identify by block number)		
FIELD	GROUP	SUB-GROUP			
			Earthquakes in Norway, source mechanisms, regional attenuation, synthetic seismograms		
19. ABSTRACT (Continue on reverse if necessary and identify by block number)					
<p>Three earthquakes of magnitude around 5 occurred offshore western Norway on 5 February 1986, on 8 August 1988 and on 23 January 1989. These earthquakes, representing the highest seismic activity level in this area for at least 30 years, were all felt by people over most of southern and central Norway. Focal mechanism solutions for these earthquakes indicate thrust faulting along N-S to NNE-SSW striking fault planes, in response to NW-SE compressional stress, most probably of plate tectonic origin.</p> <p>A number of high quality digital recordings of the ground motions at various distances from these and other recent earthquakes in Norway have shown that source spectral as well as wave attenuation characteristics in this area are reasonably consistent with what has been derived from other intraplate areas.</p>					
20. DISTRIBUTION/AVAILABILITY OF ABSTRACT <input type="checkbox"/> UNCLASSIFIED/UNLIMITED <input type="checkbox"/> SAME AS RPT <input type="checkbox"/> DTIC USERS			21. ABSTRACT SECURITY CLASSIFICATION UNCLASSIFIED		
22a. NAME OF RESPONSIBLE INDIVIDUAL James Lewkowicz			22b. TELEPHONE (Include Area Code) (617) 377-3028		22c. OFFICE SYMBOL GL/LWH

DD Form 1473, JUN 86

Previous editions are obsolete

SECURITY CLASSIFICATION OF THIS PAGE

Unclassified

Preface

Under Contract No. F49620-C-89-0038, NTNF/NORSAR is conducting research within a wide range of subjects relevant to seismic monitoring. The emphasis of the research program is on developing and assessing methods for processing of data recorded by networks of small-aperture arrays and 3-component stations, for events both at regional and teleseismic distances. In addition, more general seismological research topics are addressed.

Each quarterly technical report under this contract will present one or several separate investigations addressing specific problems within the scope of the statement of work. Summaries of the research efforts within the program as a whole will be given in annual reports.

This Scientific Report No. 2 presents a manuscript entitled "Three recent larger earthquakes offshore Norway", by Roger A. Hansen, Hilmar Bungum and Alfred Alsaker. Topics addressed in the paper include focal mechanisms, regional wave attenuation, modelling using synthetic seismograms and tectonic implications.



Accession For	
NTIS GRA&I	<input checked="" type="checkbox"/>
DTIC TAB	<input type="checkbox"/>
Unannounced	<input type="checkbox"/>
Justification	
By	
Distribution/	
Availability Codes	
Dist	Avail and/or Special
A-1	

Three Recent Larger Earthquakes Offshore Norway

by Roger A. Hansen, Hilmar Bungum and Alfred Alsaker

NORSAR, P.O.Box 51, N-2007 Kjeller, Norway

ABSTRACT

Three earthquakes of magnitude around 5 occurred offshore western Norway on 5 February, 1986, on 8 August, 1988, and on 23 January, 1989. These earthquakes, representing the highest seismic activity level in this area for at least 30 years, were all felt by people over most of southern and central Norway. Focal mechanism solutions for these earthquakes indicate thrust faulting along N-S to NNE-SSW striking fault planes, in response to NW-SE compressional stress, most probably of plate tectonic origin.

A number of high-quality digital recordings of the ground motions at various distances from these and other recent earthquakes in Norway have shown that source spectral as well as wave attenuation characteristics in this area are reasonably consistent with what has been derived from other intraplate areas.

INTRODUCTION

The seismicity of the Norwegian Continental Shelf can be characterized as moderate, since no destructive earthquakes are known to have occurred there in historical times. The seismic activity is, however, high enough for earthquake hazards and loads to be considered in the design of fixed installations offshore in Norway (Norwegian Petroleum Directorate, 1987).

In order to support the development of our knowledge about the seismic activity in these areas, the petroleum industry has contributed over the last few years to the

operation of seismic surveillance networks all along Western and Northern Norway. One of the most important of these is the Northern Norway Seismic Network, SEIS-NOR, with stations from 62° to 70°N. When considering also the large investments in equipment in Norway for the purpose of more global earthquake and explosion monitoring, this provides an excellent basis for investigation of what now possibly may represent a recent surge in seismic activity.

The purpose of the present paper is to provide a seismological analysis of three of the largest local earthquakes recently recorded by these new installations, to discuss the tectonic significance of these events, and finally to discuss some of their engineering implications. The level of detail of this paper is influenced by its intent to address a wide audience. When deemed necessary, references are made to other reports or papers that treat the topics in more detail.

REGIONAL SEISMICITY

Tectonic processes are long term, and a study of such processes is therefore aided by a combined analysis of historical and recent earthquake activity. In the case of Norway, the prime motivation for such studies has been the need for improved seismic hazard analyses, resulting in a variety of scientific studies which all have contributed to our knowledge of seismicity and seismotectonics in Norway and its surrounding offshore areas (Bungum and Selnes, 1988).

A seismicity map for Norway is shown in Fig. 1. This map includes an integration of historical as well as more recent earthquakes. The main seismotectonic features as seen from the figure are as follows (Bungum et al., 1989):

- South of 63°N, the seismicity follows the Viking Graben and the coastal areas on each side of the Horda Platform, with the zones coming together at around 62°N.
- Further north (around 64°N), the seismicity divides again to either side of the Trøndelag Platform, with the Kristiansund-Bodø Fault Complex on the offshore side and the Møre-Trøndelag Fracture Zone and the Rana Fault Complex on the coastal side.
- In the Lofoten area (around 67°N), the zones join again, while further north

another zone runs in a northwesterly direction between the Lofoten Basin and the Barents Sea.

- In a broad sense, the seismicity thereby follows the (passive) continental margin over a very long distance.

With some exceptions (Havskov et al., 1989) it has been found (Bungum and Selnes, 1988) that the seismicity in these areas has been reasonably stable since systematic macroseismic data collection began in the 1880's (Muir Wood et al., 1987). Fig. 2 shows in this respect a temporal overview of the largest earthquakes in Norway and surrounding areas, beginning with a M_S 5.8 earthquake in Nordland in 1819. Since about 1885, the coverage is considered reasonably complete down to M_S 4.5, showing two time periods with somewhat higher earthquake activity, namely a 20 year period around the turn of the century, and a five year period at the end of the 1950's.

Our focus in the following will be on investigating the three largest earthquakes at the end of the 1980's in more detail.

LOCATIONS, FELT EFFECTS, AND MAGNITUDES

Detailed parameters for the three earthquakes are given in Table 1, while locations, as well as maps of felt area contours for intensities *V*, *IV* and *III* are shown in Figs. 3-5. The hypocenters are computed in each case from a large number of local and regional instrumental recordings of *P* and *S* waves (46, 68 and 34 for Events 1, 2 and 3, respectively), giving epicentral standard errors on the order of 4, 3 and 2 km. These uncertainties are smaller than what is typically found for most of the smaller earthquakes located in the same general area during the last decade (Bungum et al., 1986). For earlier instrumentally located events, such as many of those shown in Fig. 1, uncertainties could easily be of the order of 10-20 km (Husebye et al., 1978), and even larger for some of the older macroseismically located historical earthquakes (Muir Wood et al., 1987).

In Table 1 focal depths for Events 1 and 2 are indicated only to lower crust, based on indications from the hypocentral solutions using the computer program HYPOELLIPSE (Lahr, 1984). In addition, about ten reported depth phases (*pP*

and sP) for Event 2 at teleseismic distances indicate a focal depth between 21 and 27 km. For Event 3, some near-field recordings provide a precise estimate of about 26 km quite close to (possibly just below) the crust-mantle interface (Klemperer, 1988). Focal depths of this order (15-35 km) are commonly observed in Norway (Bungum et al., 1989), and there is now increasing evidence for focal depths near the Moho discontinuity also in many other intraplate areas (Chen, 1988).

The felt area information as presented in Figs. 3-5 is the best source of information about the size of earthquakes when instrumental data are not available. It is still important to compute magnitude in this way for recent earthquakes in order to tie them in to the historical seismicity. As a part of a major reanalysis of historical seismicity in Norway, Muir Wood and Woo (1987) developed the following relationships between surface wave magnitude M_S and felt areas (in km^2) corresponding to intensity levels *III* and *IV*:

$$M_S = 0.95 + 0.69 \cdot \log A_{III} + 6 \cdot 10^{-7} A_{III} \quad (1)$$

$$M_S = 1.57 + 0.63 \cdot \log A_{IV} + 7 \cdot 10^{-7} A_{IV} \quad (2)$$

These relations were developed on the basis of some calibration events for which both instrumentally determined M_S and felt area estimates were available. In using these relations with felt areas as estimated from Figs. 3-5 we find, as shown in Table 1, M_S values of 4.9, 5.3 and 5.1 for the three events, respectively. Such M_S magnitudes, from felt areas, have been derived also for all of the larger earthquakes shown in Figs. 1-2, insuring that the whole catalogue is internally consistent.

Also given in Table 1 are some other magnitude estimates for these earthquakes. As one might expect, global network m_b estimates are higher than our M_S values, while moment magnitudes M_W are more consistent.

FOCAL MECHANISM SOLUTIONS

Focal mechanism solutions for two of the three earthquakes proved to be quite difficult to obtain using the conventional first motion analysis. There either were not enough data to well constrain the nodal planes (as was the case for Event 1), or errors were introduced in the take-off angles from the source due to misinterpretation

of the travel path of the seismic phase because of the complicated geometry of the crust-mantle interface (as was the case for Event 3).

Since Events 1 and 3 were found to have produced fairly simple and well recorded long period surface waves, an approach of source mechanism retrieval was adopted that combines broad-band waveform modelling with the more conventional first motion analysis. The method consists of low pass filtering the broad-band records from the NORESS array (NRS) and Kongsberg (KONO) to emphasize the low frequency waves up to about 6 seconds period and then matching the waveforms to synthetic seismograms computed for a given earth structure and source mechanism. Green's functions were computed using the Locked Mode Approximation method of Harvey (1981) for a crust-mantle structure derived from Mykkeltveit (1980) for the crust and Stuart (1978) for the upper mantle. A more detailed description of the waveform modelling procedure is beyond the scope of this paper and will be presented in a subsequent paper (Hansen, 1989).

The results of this modelling are illustrated in Fig. 6 and 8 for Events 1 and 3, respectively. Three-component seismograms recorded at NRS for each event are shown after filtering and rotation to vertical, radial, and transverse components. The corresponding synthetic seismograms are shown just below the observed ones. The method was first applied to Event 3 where the best results were obtained. To the right of Fig. 6 and 8 are the focal mechanism drawings (lower hemisphere stereographic projections) for the nodal planes obtained from the waveform modelling together with the first motion data. It is obvious that the first motion data are to some extent discordant, either due to incorrect readings or false interpretations. Experimenting with different velocity models for location, and varying the source depth failed to improve the interpretation of the first motion data. However, they were useful in helping to discriminate between say two different waveform solutions and serve to supply constraints on further interpretation of velocity models in the area.

Due to the complexity of the crust and upper mantle structure in the vicinity of the earthquakes, it was necessary to explore the effect of the assumed velocity structure on the low frequency waveform modelling. Since we are observing phases with wavelengths on the order of 20 kilometers and longer, much of the complexity effecting the high frequency first motion data is smoothed out. The structures

used for computing synthetic seismograms therefore reflected the average, and more homogeneous, properties sampled along the majority of the travel path from the earthquake to the receiving stations. By observing the change in the synthetic waveforms as a function of structural model and earthquake source depth it was verified that the solutions for the focal mechanisms and source depths are quite robust. Variations in the compression and tension axes of the focal sphere were found to be less than about 5 degrees due to changes in velocity models for a single station solution, and were improved with the inclusion of a second three-component station (KONO). It was also found that source depths could be verified from the modelling to a precision of about ± 5 km.

For Event 1 (Fig. 6), the waveform fit at station NRS is excellent except for a time shift in the transverse component. It is seen from the focal mechanism plot that the fault plane solution would be difficult to obtain from first motion data alone. In fact, an earlier interpretation of the first motion data of this event indicated a normal fault with a near vertical axis of maximum compression. However, the waveform modelling shown here for this event completely rules out this type of solution. Instead, the solution for this earthquake clearly indicates oblique thrust faulting in response to a regional stress field exhibiting NW-SE horizontal compression.

For Event 2, a similar amplitude modelling has not been feasible because of the very different character of the long period waveforms as illustrated in Fig. 7. The complex seismograms are likely a result of the rapidly changing crustal structure between Event 2, which is the farthest out to sea, and the seismometer located in south-eastern Norway (Hamar and Hjelle, 1984). In this case, a solution using first motions only is given in Fig. 7, where a combination of local and teleseismic data helps in constraining the nodal planes. The solution (see Table 1) shows, as for Event 1, a thrust mechanism in response to NW-SE compression, but with somewhat different faulting parameters.

It is of interest here to point out that such a reliable fault plane solution is only possible because of the newly installed stations in Northern Norway. It can be seen from Fig. 7 that the northeasterly striking plane is only constrained by the stations whose azimuths vary from about 40° through about 90°. These are the stations of the SEISNOR network and the ARCESS array. The sense of first motion changed from dilatation to compression through the middle of this network

of stations, allowing for a well constrained fault plane solution.

For Event 3 (Fig. 8), the solution again indicates thrust faulting in response to NW-SE compression. Since there were two seismic stations within about 50 km from the earthquake, both *P* and *S* type seismic phases were usable for constraining the depths of the main shock and several aftershocks. Since the locations of these aftershocks indicate a plane dipping to the southeast it is likely that the fault plane for the main shock is the one with a northeast strike dipping to the southeast.

SOURCE SPECTRA AND SEISMIC MOMENTS

Source displacement spectra are obtained in general by first computing observed displacement spectra, and then correcting for path effects (geometrical spreading and anelastic attenuation). In order for such estimates to be reliable they need near-field data recorded over a broad band of frequencies, and with a high dynamic range. Reliable near-field data are scarce anywhere, and in particular in intraplate areas such as Norway. We do, however, have recording systems available that fulfill the other requirements. These are one three-component broad band (intermediate period) station at NORESS (all three events) and two strong-motion instruments (accelerographs) at Molde and Sulen (Event 2 only).

Given that we have independent information on the sense of faulting, the source spectrum can be interpreted in terms of "standard" earthquake source models. The most commonly used source model is the "Brune" model (Brune, 1970; 1971), developed from a study of shear waves radiated by a sudden drop in shear stress over a circular region in an infinite elastic solid. Here the spectrum is characterized by a fairly simple shape, where the parameters of interest are a low frequency asymptote Ω_0 , a corner frequency f_0 and a high frequency roll-off that is linear with a slope proportional to ω^2 (12 dB/octave).

The observed displacement spectra Ω_ω estimated here were obtained by first rotating the time series to yield the radial and transverse components, followed by Fourier transforming, highpass filtering (to avoid noise problems with the inverse FFT to obtain ground displacement time series), correcting for the instrument response, and then integrating to displacement (from acceleration or from velocity, depending on type of instrument).

From the observed displacement spectrum, the source spectrum as a function of angular frequency $\omega = 2\pi f$ is estimated simply by correcting for path effects all the way back to the source, as follows:

$$M_\omega = 4\pi\rho v^3(GPS)^{-1}\Omega_\omega \quad (3)$$

where ρ is the density of the material, v is the seismic velocity of the wave being analyzed, G accounts for geometrical spreading (spherical up to 100 km, then cylindrical), S is a factor that accounts for the free surface amplification (2.0), radiation pattern coefficient (0.6), and possible vectorial partitioning of energy ($\sqrt{2}$), and P is a path correction term that includes anelastic attenuation:

$$P = \exp(\omega R/vQ) \quad (4)$$

where R is epicentral distance and $Q = Q(f)$ is a frequency dependent quality factor. Two quite different relationships have previously been used to account for anelastic attenuation in Norway, one from Sereno et al. (1988) and the other from Kvamme and Havskov (1989). Both relationships were based on local and regional recordings of smaller earthquakes from Norway and surrounding areas. More recently, a new relationship has been developed by Dahle et al. (1989), based on a large amount of intraplate strong motion recordings from earthquakes with magnitudes more appropriate for the present application. These three relationships are as follows (the last one slightly simplified here):

$$Q = 560f^{0.26} \quad (\text{Sereno et al., 1988}) \quad (5)$$

$$Q = 120f^{1.1} \quad (\text{Kvamme and Havskov, 1989}) \quad (6)$$

$$Q = 360 + 103f^{1.2} \quad (\text{Dahle et al., 1989}) \quad (7)$$

It can be seen from these equations that (7) is reasonably close to (6) for high frequencies and quite close to (5) for low frequencies. In applying these relationships in Equation (3), however, we find that frequency dependencies as given by (6) or (7) are needed in order to get source spectral slopes consistent with common models (e.g. Chael and Cromer, 1988), Q -values as given by (7) are needed at high

frequencies in order to get consistent source spectral levels from observations at different distances, while Q -values between those given by (6) and (7) are needed in order to get consistent estimates of seismic moments. A relationship averaging the ones above has therefore been used in the present analysis:

$$Q = 90 + 110f^{1.2} \quad (8)$$

In applying equation (8) in equations (3) and (4), certain parameters quantifying the source strength and spatial extent can be estimated by simply reading the spectral amplitude and the corner frequency levels. The low frequency asymptote here is in fact the seismic moment M_0 , which is the strength of the equivalent double couple source.

The corner frequency f_0 (inversely proportional to source radius) yields a measure of the size of the fault surface that moved during the earthquake. The Brune model assumes this fault surface to be circular, with a radius given by a ratio proportional to the wave speed v divided by the corner frequency f_0 .

The Brune source model also allows for the estimation of the stress drop (or amount of accumulated strain-energy released by the earthquake) from the parameters of seismic moment and fault area. Other estimates such as amount of slip on the fault can be calculated from simple formulae. Further, estimates of energy radiated by the source can be made from the squared velocity trace and then related to an apparent stress estimate for the event (Aki, 1966; Wyss, 1970). Finally, to better relate these spectral parameterizations to more commonly used magnitude estimates the more robust measure of absolute strength of the source given by the seismic moment M_0 (in Newton-meters), has been expressed as a moment magnitude, M_W , by this simple formula of Hanks and Kanamori (1979):

$$M_W = 2/3 \log M_0 - 6.0 \quad (9)$$

By analyzing the S (L_g) phases observed from the three events at different stations in this way, we have obtained source displacement spectra as shown in Figs. 9-11 and associated source parameters as given in Table 1. To be consistent, the interpreted Brune source spectra are fitted by eye using the NORESS data only (in Figure 10, spectra from Molde and Sulen are also plotted indicating a somewhat lower low-frequency level), and with an ω^2 slope at higher frequencies. The resulting

moment levels and corner frequencies are given in Table 1 along with the computed stress drops, source radii, and average fault displacements. It is interesting to note that the stress drops average at 10 MPa, a value which is commonly observed. It should be noted here that an essentially unresolved discussion still exists with respect to whether or not stress drop is higher for earthquakes in intraplate areas than in plate margin areas (Kanamori and Anderson, 1975; Somerville et al, 1987), and with respect to whether or not stress drop is independent of seismic moment (Nuttli, 1983).

It should be emphasized that this estimation of source displacement and thereby its low frequency asymptote M_0 is very dependent on the models used for anelastic attenuation (Q), in particular for low frequencies. Even though some Q models already have been published for Norway as discussed above, a lot more research is needed until a model is established which gives us sufficiently reliable seismic moment estimates when obtained from data recorded at regional distances over say 100 km.

The model used for geometrical spreading is also important (cf. Street et al, 1975; Herrmann and Kijko, 1983), because the spreading term, even up to distances of several hundred kilometers, contributes much more to the total attenuation than the anelastic term, and also because different spreading models used could make a large difference at larger regional distances. For most models (for L_g waves) the latter point is reduced to a question of at what distance (100 km in the present study) the geometrical spreading changes from spherical to cylindrical, which in turn depends on crustal structure and focal depth. The answer to this question is not firmly established for any area. In Q studies, some assumption on geometrical spreading is usually a prerequisite, and therefore strongly influences the results. It is therefore quite encouraging that we have obtained such consistent results between the moment magnitudes and the various estimates of surface wave magnitudes for these events.

TECTONIC IMPLICATIONS

The three earthquakes studied here are among the largest ones in this area for more than 100 years (Ambraseys, 1985; Muir Wood et al., 1987; Bungum and

Selnes, 1988), as seen from Figs. 1-2. Specific events in the same magnitude range to compare with are the following:

Year/date	Lat.(°N)	Long.(°E)	M_s
1866/03/09	65.2	6.0	5.7
1892/05/15	61.4	5.1	5.2
1895/02/05	65.0	6.0	5.3
1955/06/03	61.9	4.1	5.2

Of these earthquakes, which all are analyzed in detail in terms of felt effects, it seems that the one in 1866 is definitely greater than the recent ones, and possibly also the one in 1895 (see also Ambraseys and Elnashei, 1988). The other two are closer in size, and by comparing felt area information it is possible that the 1955 event is indeed smaller (M_s 5.2 for that event is an instrumental value). In that case, the 1988 Møre Basin earthquake is the largest one in this part of the Norwegian Continental Shelf since 1895.

The focal mechanism solutions for Events 1-3 all have significant reverse (thrust) components, in response to NW-SE compression. This is quite consistent with the direction of the "ridge push" force which now often is assumed to be responsible for the regional stress field in these areas (cf. Gregersen and Basham, 1989; Bungum et al., 1989). The fact that three recent larger earthquakes, with their greater regional tectonic significance, are so consistent with this model is indeed a very strong evidence in its support.

Double couple focal mechanism solutions such as those obtained here leave an ambiguity with respect to which of the two fault planes is the actual rupture plane. This ambiguity can be resolved only by use of additional, normally geologic, data. Such data in this case indicates in general a predominance of NS or NE-SW striking faults, which in fact does not exclude any of the nodal planes in Figs. 6-8. A more detailed geological analysis of the epicentral areas is therefore needed in order to resolve this question. For Event 3, however, the lineation of aftershocks (as mentioned above) clearly suggests the southeast dipping plane.

It is usual to find that earthquakes of the size studied here are followed by a large number of aftershocks ranging in magnitude from about one unit lower than the main shock and down to the minimum detection level. Such aftershocks were observed for both Event 1 (Chael and Cromer, 1986) and for Event 3, while none were found for Event 2 (8 August 1988). For Event 2, the signal to noise ratio for

the earthquake, combined with some simple scaling relations on earthquake spectra (e.g. Evernden et al., 1986), tell us that aftershocks as low in magnitude as 2.5 to 3.0 should have been detected if they occurred.

Another example by contrast is the Meløy sequence of earthquakes (Bungum et al., 1979). This sequence produced literally thousands of earthquakes over a time period of a few months and then rapidly decayed away. However, the largest event in the Meløy sequence was only 3.2, which characterizes a swarm rather than a main shock/aftershock sequence.

Since the faulting mechanisms as well as the focal depths in these three cases are reasonably similar, it is likely that the lack of aftershocks for Event 2, the largest of the three, is tied to differences in the local geological conditions in the Møre Basin. For example, in the Møre Basin, up to about 10 km of sediments lie above the basement rocks (Hamar and Hjelle, 1984). The other two events occurred near the areas where the sedimentary basins are separated from the crystalline massifs on the landward side. Also of significance to Event 2 is that the direction of horizontal compression obtained from the focal mechanism, in contrast to Events 1 and 3, deviates slightly from the direction of expected ridge-push forces.

ENGINEERING IMPLICATIONS

The Norwegian Continental Shelf is characterized by a moderate level of seismicity (Bungum et al., 1989). This means that the seismicity is high enough to be of concern in the design of offshore installations (Norwegian Petroleum Directorate, 1987) while at the same time low enough to create special problems in the estimation of earthquake hazards and loads for this area (Bungum and Dahle, 1989).

One of the main sources of uncertainty in this respect is the model used for wave attenuation, especially in the near field. The classical way of obtaining such models for attenuation relations is through a regression analysis of strong motion data with a sufficient coverage in magnitude and distance. Since large earthquakes are rare in Norway, with no known destructive earthquake, this approach is not possible here. By including data from other and tectonically comparable areas, however, the approach is viable, as shown recently by Dahle et al. (1989).

In a recent major Norwegian earthquake hazard study (Bungum and Selnes,

1988), a solution to this problem was sought in terms of a combination of attenuation relations developed from data recorded in tectonically similar areas, and relations developed on a more theoretical basis.

An interesting approach for a further improvement in attenuation models is now available in terms of the so-called "calibrated theoretical" method of ground motion predictions based on a random-vibration approach (e.g., Boore and Atkinson, 1987; Toro and McGuire, 1987). In this approach, the observed ground motion spectra are predicted based on a simple model for the source spectrum, and in a way almost inversely to what was done above in the computation of source displacement spectra. One of the advantages with this approach is that it can utilize all available seismometer recordings from earthquakes of small and moderate magnitudes in the development of parameters for the prediction models. What is needed is a correction for instrument response, a conversion from displacement to acceleration, and the subsequent computation of Fourier spectra and/or response spectra.

An example of such Fourier spectra is given in Fig. 12, where acceleration spectra are computed (units of m/s) for NORESS three-component broad band recordings of Event 2 (8 August 1988). The figure also includes noise spectra as well as theoretical predictions using the random-vibration approach based on parameters given in the figure caption. In spite of the fact that these parameters have been derived independently of the event for which the predictions are computed, the fit is almost perfect. This should be considered coincidental, however, since the parameters used have not been derived through a systematic analysis and therefore not necessarily would predict amplitudes equally well for other earthquake magnitudes and wave paths.

One of the reasons why Event 2 is important within this context of ground motion predictions is that the event is large enough to provide valuable constraints on the possible non-linearity of the moment/magnitude relations, as well as for other parameters that scale with magnitude. At the same time, the earthquake also represents the first case of well-recorded accelerograms from a local earthquake of this size in Norway (unfortunately, the accelerometers were not in operation at the time of Event 3). As such, the data also contributes importantly in the extensive strong motion regression analysis by Dahle et al. (1989).

A comparison between the Event 2 observed ground motions with what is pre-

dicted by the Dahle et al. (1989) wave attenuation model is shown in Fig. 13. The parameter used there is peak ground acceleration PGA (at 5 percent damping), historically one of the most important ground motion parameters used in earthquake engineering. The curve is generated for an M_S 5.3 earthquake, and the two points are PGA values from Molde and Sulen. It is seen from the figure that the observed points are somewhat below the model predictions of the order of one standard deviation.

While PGA represents an asymptotic value of acceleration for high frequencies, the ground motion values for lower frequencies are often of greater importance for the kind of engineering applications usually found on the Norwegian Continental Shelf (with periods all the way up to 6 seconds in some cases). The parameter most widely used in that case is the pseudo-relative velocity PSV, which describes (as does PGA) the response of a single degree of freedom oscillator with some level of damping (usually around 5 percent) to the ground motion.

It should be kept in mind here that these response spectral velocities, or pseudo-relative velocities PSV, are distinctly different from Fourier spectra, which describe the ground motion itself. Both, however, come in units of velocity provided that the input is in units of acceleration.

Such acceleration records, in processed form, are shown in Fig. 14 for Event 2 (8 August 1988), as recorded at the Molde and Sulen stations. The processing here (eg., Shyam Sunder and Connor, 1982) includes instrument corrections as well as a very careful bandpass filtering for the purpose of signal-to-noise ratio enhancement.

At the bottom of Fig. 14 the PSV spectra for the Molde and Sulen accelerometer recordings are shown together with predictions (smooth curves) based on the Dahle et al. (1989) attenuation model. The fit between the observed and the predicted spectral forms is good, with predictions again being somewhat higher than observations. This deviation, however, is not large enough to indicate any systematic deviation between earthquakes in Norway and other intraplate areas, since only one event is represented in the comparison, and since a very large scatter is a general characteristic of such data.

In conclusion, these analyses of the largest earthquakes in Norway far at least 30 years has shown that inferred stress directions (NW-SE compression) are consistent with those expected from the "ridge-push" effect, and that source spectral shapes,

stress drops, and levels of ground motion excitation are reasonably consistent with what has been observed in other intraplate areas.

ACKNOWLEDGEMENTS

This research was supported in part by the SEISNOR project operated by the University of Bergen and NORSAR (supported by BP, Conoco, Elf Aquitaine, Esso, Mobil, Norsk Hydro, Norske Shell, Phillips, Saga Petroleum, Statoil and Total), and by the Western Norway Seismic Network project operated by the University of Bergen (supported by Norsk Hydro, Norske Shell and Statoil). This research was also supported by the Advanced Research Projects Agency of the U. S. Department of Defense and was monitored by the Air Force Office of Scientific Research under Contract No. F49620-89-C-0038. Support for one of the authors (RAH) also came in part from a grant from the Norwegian Marshall Fund of the Norway-America Foundation. The authors thank Peter Marrow of the British Geological Survey for supplying important data from their stations in Western Norway, Anders Dahle and Leif B. Kvamme for helpful discussions, and Willy Aspinall for a helpful review.

REFERENCES

- Aki K. (1966) Generation and propagation of G waves from the Niigata earthquake of June 16, 1964, 2. Estimation of earthquake movement, released energy, and stress-strain drop from G wave spectrum, *Bull. Earthq. Res. Inst. (Japan)*, **44**, 23-88.
- Ambraseys N.N. (1985) The seismicity of western Scandinavia, *Journ. Earthq. Eng. and Struct. Dyn.*, **13**, 361-399.
- Ambraseys N.N. and Elnashei A.S. (1988) The Norwegian Sea Earthquake of 8 August 1988, *Europ. Earthq. Eng.*, **II**, 3, 53-54.
- Boore D.M. and Atkinson G.M. (1987) Stochastic prediction of ground motion and spectral response parameters at hard-rock sites in eastern North America. *Bull. Seism. Soc. Am.*, **77**, 440-467.
- Brune J.N. (1970) Tectonic stress and spectra of seismic shear waves from earthquakes, *J. Geophys. Res.*, **75**, 4997-5009. (Correction, *J. Geophys. Res.*, 1971, **76**, 5002.)
- Bungum H., Alsaker, A., Kvamme, L.B. and Hansen R.A. (1989) Seismicity and seismotectonics of Norway and nearby continental shelf areas. In preparation, NORSAR, Kjeller, Norway.
- Bungum H. and Dahle A. (1988) On the determination of seismic hazards in Norwegian Continental Shelf areas. In: *Earthquakes at North Sea Passive Margins: Neotectonics and Postglacial Rebound*, (ed. by S. Gregersen and P.W. Basham), pp. 665-677. Kluwer Academic Publishers, Dordrecht.
- Bungum H., Havskov J., Hokland B.K. and Newmark R. (1986) Contemporary seismicity of northwest Europe, *Ann. Geophys.*, **4**, B5, 567-576.
- Bungum H., Hokland B.K., Husebye E.S. and Ringdal F. (1979) An exceptional intraplate earthquake sequence in Meløy, Northern Norway, *Nature*, **280**, 32-35.
- Bungum H. and Selnes P.B. (eds.) (1988) *Earthquake Loading on the Norwegian Continental Shelf - Summary Report*, 38 pp. Norwegian Geotechnical Institute, Oslo.

- Chael E.P. and Cromer R.P. (1988) High-frequency spectral scaling of a main shock/aftershock sequence near the Norwegian coast, *Bull. Seism. Soc. Am.*, **78**, 561-570.
- Chen W.-P. (1988) A brief update on the focal depths of intracontinental earthquakes and their correlations with heat flow and tectonic age, *Seism. Res. Lett.*, **59**, 263-272.
- Dahle A., Bungum H. and Kvamme L.B. (1989) Attenuation models inferred from intraplate earthquake recordings. In preparation, NOR-SAR, Kjeller, Norway.
- Evernden J.F., Archambeau C.B. and Cranswick E. (1986) An evaluation of seismic decoupling and underground nuclear test monitoring using high-frequency seismic data, *Rev. Geophys.*, **24**, 143-215.
- Gregersen S. and Basham P.W. (eds.) (1988) *Earthquakes at North Sea Passive Margins: Neotectonics and Postglacial Rebound*, 716 pp. Kluwer Academic Publishers, Dordrecht.
- Hamar G.P. and Hjelle K. (1984) Tectonic framework of the Møre Basin and the northern North Sea. In: *Petroleum Geology of the North European Margin*, (ed. by A.M. Spencer et al.), pp. 349-358, Norwegian Petroleum Society, Graham and Trotman, London.
- Hanks T. and Kanamori H. (1979) A moment magnitude scale, *J. Geophys. Res.*, **84**, 2348-2350.
- Hansen R.A. (1989) Source parameters of Norwegian earthquakes recorded at local and regional distances (abstract), Proceedings of the 25th General Assembly of the International Association of Seismology and the Physics of the Earth's Interior. Manuscript in preparation.
- Harvey D. (1981) Seismogram synthesis using normal mode superposition: the locked mode approximation, *Geophys. J. R. astr. Soc.*, **66**, 37-61.
- Havskov J. and Bungum H. (1987) Source parameters for earthquakes in the northern North Sea, *Nor. Geol. Tidsskr.*, **67**, 51-58.
- Havskov J., Lindholm C.D. and R.A. Hansen (1989) Temporal variations in North Sea seismicity. In: *Earthquakes at North Sea Passive Margins: Neotectonics and Postglacial Rebound*, (ed. by S. Gregersen

- and P.W. Basham), pp. 413-427. Kluwer Academic Publishers, Dordrecht.
- Herrmann R.B. and Kijko A. (1983) Modeling some empirical component L_g relations, *Bull. Seism. Soc. Am.*, **73**, 157-171.
- Husebye E.S., Bungum H., Fyen J. and Gjøystdal H. (1978) Earthquake activity in Fennoscandia between 1497 and 1975 and intraplate tectonics, *Nor. Geol. Tidsskr.*, **58**, 51-68.
- Kanamori H. and Anderson D.L. (1975) Theoretical bases of some empirical relations in seismology, *Bull. Seism. Soc. Am.*, **65**, 1073.
- Klemperer S.L. (1988) Crustal thinning and nature of extension in the northern North Sea from deep seismic reflection profiling, *Tectonics*, **7**, 903-821.
- Kvamme L.B. and Havskov J. (1989) Q in Southern Norway, *Bull. Seism. Soc. Am.*, in press.
- Lahr J. C. (1984) HYPOELLIPSE/VAX: a computer program for determining local earthquake hypocentral parameters, magnitude, and first motion pattern, *U.S. Geol. Surv., Open-File Rept.*, **84-519**, 67 pp.
- Muir Wood R. and Woo G. (1987) *The Historical Seismicity of The Norwegian Continental Shelf*, Earthquake Loading on the Norwegian Continental Shelf (ELOCS) Report 2-1, 117 pp. Norwegian Geotechnical Institute, Norway.
- Muir Wood R., Woo G. and Bungum H. (1987) The history of earthquakes in the northern North Sea. In: *Historical Seismograms and Earthquakes of the World* (ed. by W.K.H. Lee, H. Meyers and K. Shimazaki), pp. 297-306, Academic Press, San Diego.
- Mykkeltveit S. (1980) A seismic profile in southern Norway, *Pageoph.*, **118**, 1310-1325.
- Norwegian Petroleum Directorate (NPD) (1987) *Retningslinjer for fastsettelse av laster og lastvirkninger*, 38 pp. Norwegian Petroleum Directorate, Stavanger.
- Nuttli O.W. (1983) Empirical magnitude and spectral scaling relations for mid-plate and plate margin earthquakes, *Tectonophysics*, **93**, 207.

- Sereno T.J., Bratt S.R. and Bache T. (1988) Simultaneous inversion of regional wave spectra for attenuation and seismic moment in Scandinavia, *J. Geophys. Res.*, **93**, 2019-2035.
- Shyam Sunder S. and Connor J. (1982) A new procedure for processing of strong-motion earthquake signals, *Bull. Seism. Soc. Am.*, **72**, 643-551.
- Somerville P.G., McLaren J.P., LeFevre L.V., Burger R.W. and Helmburger D.V. (1987) Comparison of source scaling relations of eastern and western North American earthquakes, *Bull. Seism. Soc. Am.*, **77**, 322-346.
- Street R.L., Herrmann R.B. and Nuttli O.W. (1975) Spectral characteristics of the L_g wave generated by Central United States earthquakes, *Geophys. J. R. astr. Soc.*, **41**, 51-63.
- Stuart G.W. (1978) The upper mantle structure of the North Sea region from Rayleigh wave dispersion, *Geophys. J. R. astr. Soc.*, **52**, 367-382.
- Toro G.R. and McGuire R.K. (1987) An investigation into earthquake ground motion characteristics in eastern North America., *Bull. Seism. Soc. Am.*, **77**, 468-489.
- Wyss M. (1970) Stress estimates for South American shallow and deep earthquakes, *J. Geophys. Res.*, **75**, 1529-1544.

Event No.	1	2	3
Year/Month/Day	1986/2/5	1988/8/8	1989/1/23
Latitude (°N)	62.71	63.68	61.97
Longitude(°N)	4.69	2.44	4.42
Focal depth (km)	15-30	20-30	24-28
Felt area A_{IV} (1000 km ²)	140	320	245
M_S (felt area A_{IV})	4.9	5.3	5.1
Felt area A_{III} (1000 km ²)	310	580	460
M_S (felt area A_{III})	4.9	5.3	5.1
m_b (NEIS)	5.0 (4)	5.7 (70)	5.5
M_S (NEIS)	4.4 (6)	5.3 (13)	5.1
Seismic moment (10 ¹⁶ Nm)	1.3	8.0	6.0
M_W (moment magnitude)	4.7	5.3	5.2
Corner frequency (Hz)	1.4	1.0	1.0
Stress drop (MPa)	5.5	12.4	12.3
Source radius (km)	1.0	1.4	1.3
Average slip (cm)	12	39	35
P-axis strike (°)	303	277	124
P-axis plunge (°)	10	5	8
T-axis strike (°)	198	31	239
T-axis plunge (°)	55	77	72

Table 1

Table Captions

Table 1: Source parameters for the three earthquakes analyzed in this paper: Event number; date; latitude; longitude; focal depth; felt area and M_S (from felt area) for MSK intensity levels *IV* and *III*; network determinations of m_b and M_S from the U.S. National Earthquake Information Service NEIS (number of stations in parentheses); seismic moment; moment magnitude; corner frequency, stress drop (1 MPa = 10 bars), source radius, and average slip across the fault, based on a Brune source model; P-axis (maximum compression) strike and plunge; and T-axis (minimum compression) strike and plunge.

Figure Captions

Fig. 1: Earthquakes 1800-1989 in Norway and surrounding areas. The event locations for 1800-1954 are mostly based on macroseismic (felt) data, supplemented with some instrumental records from a sparse international network of stations, for the time period 1955-1979 the locations are mostly instrumental, supplemented with some macroseismic data, while the time period 1980-1989 has locations mostly based on data from regional and local seismological networks (Bungum et al., 1989). Major faults, fracture and graben systems are indicated on the figure (Bungum and Selnes, 1988), and the heavy line from south to north offshore indicates 500 m water depth, corresponding roughly to the edge of the continental shelf. Earthquake symbol size is proportional to magnitude as shown by the legend, and different symbols are used for the three time periods.

Fig. 2: Time-magnitude distribution of earthquakes in the area covered in Fig. 1 (mid-Atlantic ridge and Lofoten Basin excluded), and for events of M_S 4.5 and above. The three events reported on in this study are those numbered 1 through 3 on the right hand side, while other larger earthquakes include: 1819, M_S 5.8, Northern Norway; 1866, M_S 5.7, Western Norway; 1894, M_S 5.4 Lofoten Islands; 1895, M_S 5.3, Western Norway; 1904, M_S 5.4, Oslo Fjord; 1927, M_S 5.3, Northern North Sea; and 1955, M_S 5.2, Western Norway.

Fig. 3: Macroseismic map for Event 1, 5 February 1986. The epicenter is indicated by a black dot, felt area contours for intensity levels *V*, *IV* and *III* (MSK scale) are shown by dashed lines, and a triangle shows the location of the NORESS station in southeastern Norway (used in the source spectral analysis in Fig. 6). The heavy line offshore indicates a water depth of 500 m (shelf edge), with 1000 and 2000 m contours further out at sea. The macroseismic data for this and the other two events reported on here have been collected and kindly provided to us by the Seismological Observatory of the University of Bergen (P. Optun), while the interpretations here are those of the authors.

Fig. 4: Macroseismic map for Event 2, 8 August 1988. Symbols and legends are

as for Event 1 (Fig. 3), and in addition the locations of the Molde and the Sulen accelerometer stations, used in the present analysis of Event 2, are also shown (see also Ambraseys and Elnashei, 1988).

Fig. 5: Macroseismic map for Event 3, 23 January 1989. Symbols and legends are as for Event 1 (Fig. 3).

Fig. 6: Focal mechanism solution from waveform modelling, Event 1, 5 February 1986. The *left* frame shows three components (vertical, radial and transverse) of NORESS broad band data together with theoretical seismograms immediately below each trace, while the *right* frame shows the focal mechanism solution used in the waveform modelling. Together with the solution, plotted in a lower hemisphere stereographic projection, are shown (but not used in the analysis) first motion polarity data, where black squares and open circles indicate compressions and dilatations, respectively. Below the solution are given the parameters for the nodal planes, for the P and T axes (maximum and minimum compressive stress), for the greatest horizontal compression and tension, and for the relative size of the horizontal deviatoric stress (for a closer explanation of these parameters see Havskov and Bungum, 1987),

Fig. 7: Focal mechanism solution from first motion data, Event 2, 8 August 1988. Symbols and legends are as for Event 1 (Fig. 6), with the important difference that no waveform modelling is done in this case (for reasons discussed in the main text). The solution therefore obtained solely on the basis of the first motion polarity data.

Fig. 8: Focal mechanism solution from waveform modelling, Event 3, 23 January 1989. Symbols and legends are as for Event 1 (Fig. 6), the only difference being that first motion data not read by the authors are indicated by plus and minus signs for compressions and dilatations, respectively.

Fig. 9: Source displacement in Nm ($1 \text{ Nm} = 10^7 \text{ dyne cm}$) vs. frequency (in Hz) for Event 1, 5 February 1986, based on NORESS (epicentral distance 428 km) three-component (vertical, radial, and transverse) broad band (IP) and high-frequency (HF) data. The heavy line indicates the "Brune" source spectrum fit by eye under

the restriction of an ω^2 slope above the corner frequency. The spectrum indicates a seismic moment of $1.3 \cdot 10^{16}$ Nm, and a corner frequency of 1.4 Hz (See Table 1).

Fig. 10: Source displacement vs. frequency for Event 2, 8 August 1988, based on NORESS (578 km) three-component broad band (IP and HF) data and Molde (288 km) and Sulen (318 km) accelerometer data. The heavy line indicates the "Brune" spectrum as in Figure 9. The spectrum indicates a seismic moment of about $8 \cdot 10^{16}$ Nm, and a corner frequency of 1.0 Hz (See Table 1).

Fig. 11: Source displacement vs. frequency for Event 3, 23 January 1989, based on NORESS (415 km) three-component broad band (IP and HF) data. The heavy line indicates the "Brune" spectrum as in Figure 9. The spectrum indicates a seismic moment of about $6 \cdot 10^{16}$ Nm, and a corner frequency of 1.1 Hz (See Table 1).

Fig. 12: Fourier spectra of acceleration for NORESS three component (vertical, radial and transverse) ground motion seismograms (corrected for instrument response) from the Event 2 (8 August 1988), together with theoretical amplitude predictions (black squares) using the random-vibration technique discussed in the main text. The predictions are based on a 'Brune' source model, a stress drop of 10 MPa, geometrical spreading as in the source spectral analysis above, and anelastic attenuation as given by Kvamme and Havskov (1989). Below are given similar spectra for the preceding noise, showing an excellent signal-to-noise ratio of (60-70 dB). The data are converted (differentiated) to acceleration before spectral estimation.

Fig. 13: Peak ground acceleration PGA (5 percent of critical damping) versus distance (with standard deviations) for an M_S 5.3 earthquake, as taken from the wave attenuation relation of Dahle et al. (1989), together with observed PGA at stations Molde and Sulen for Event 2 (8 August 1988).

Fig. 14: Processed acceleration records from Molde (left) and Sulen (right) for Event 2 (8 August 1988). Below are plotted PSV (pseudo-relative velocity) response spectra and predictions (smooth curve) based on the Dahle et al. (1989) wave attenuation model.

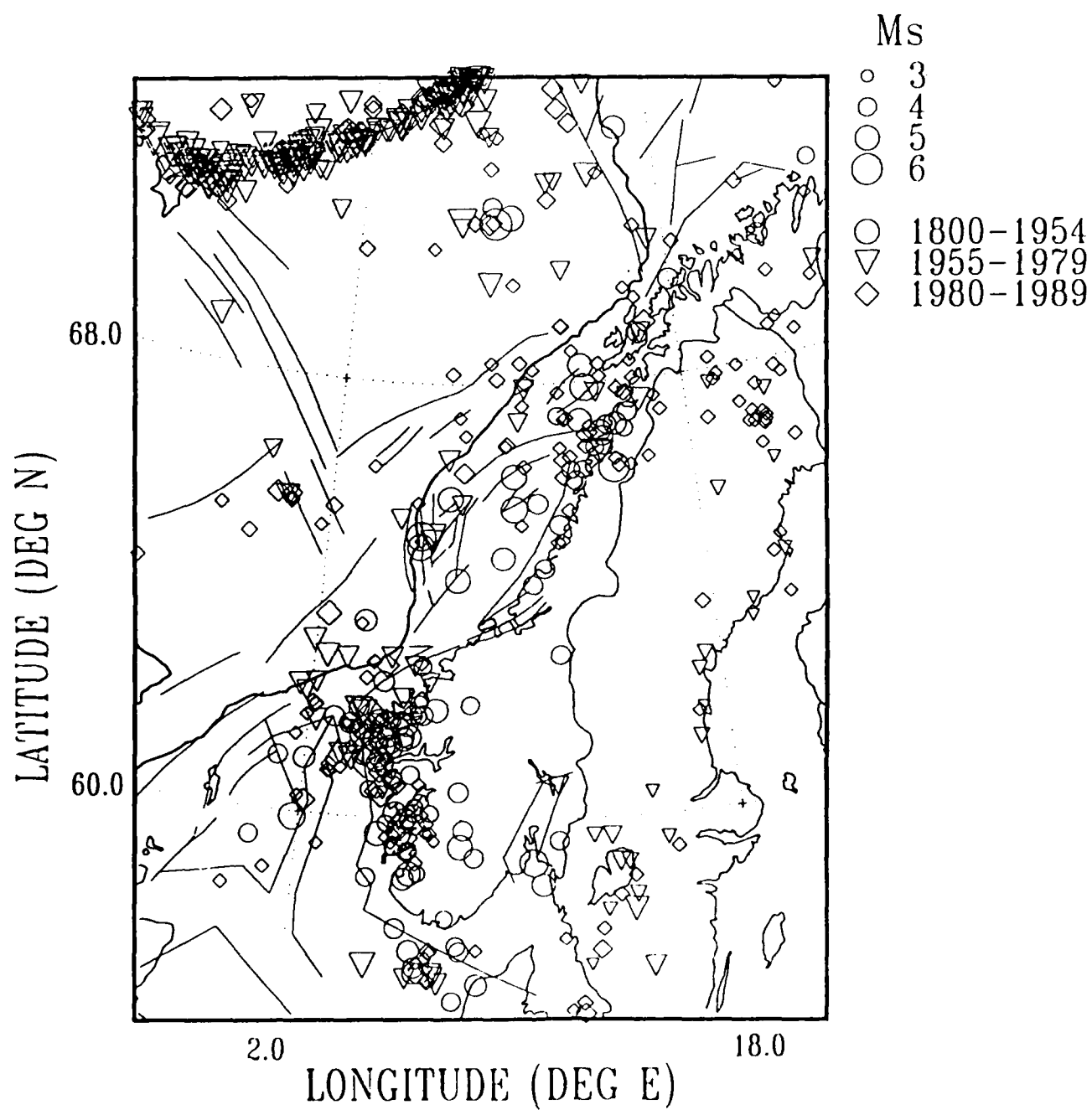


Figure 1

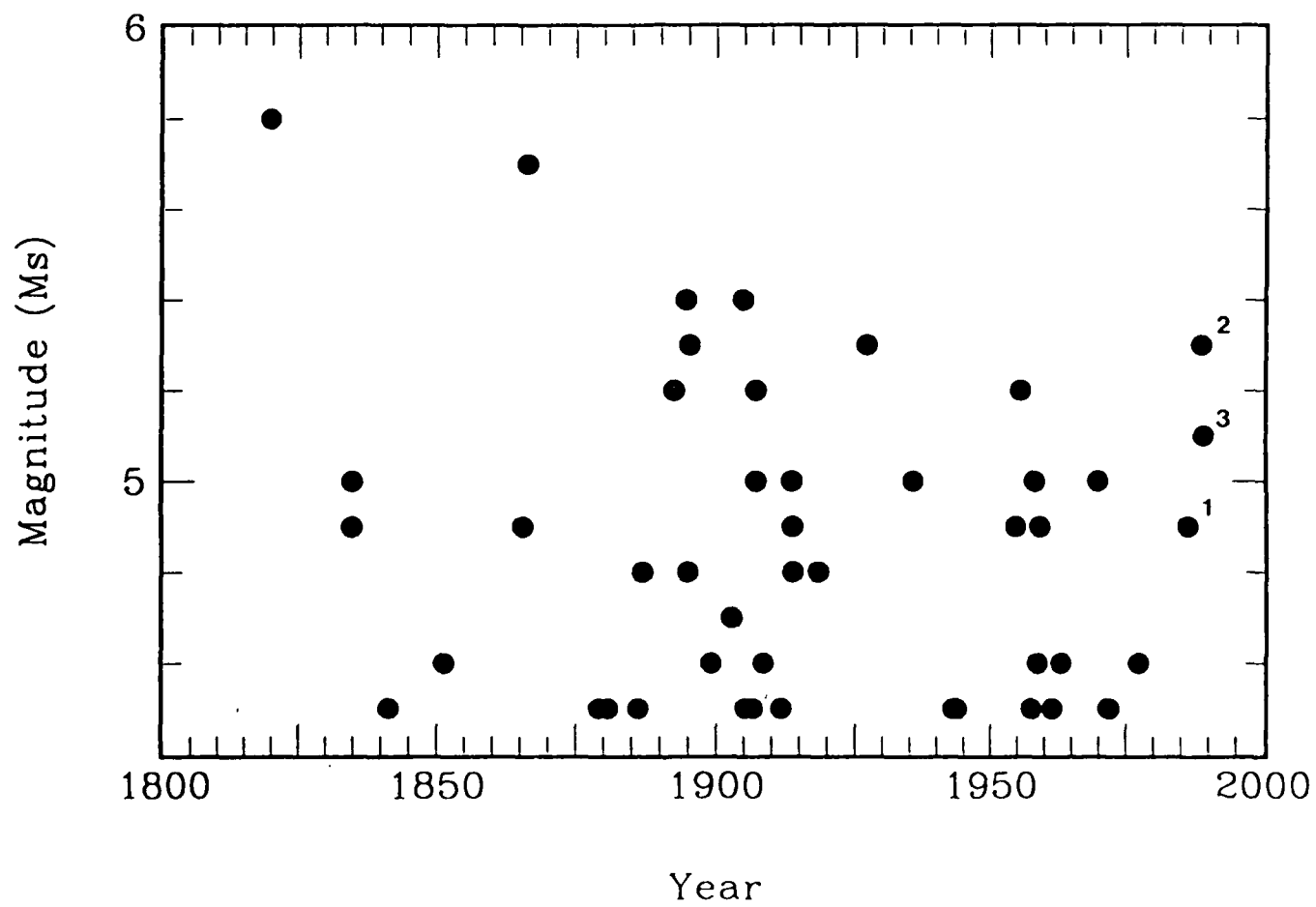


Figure 2

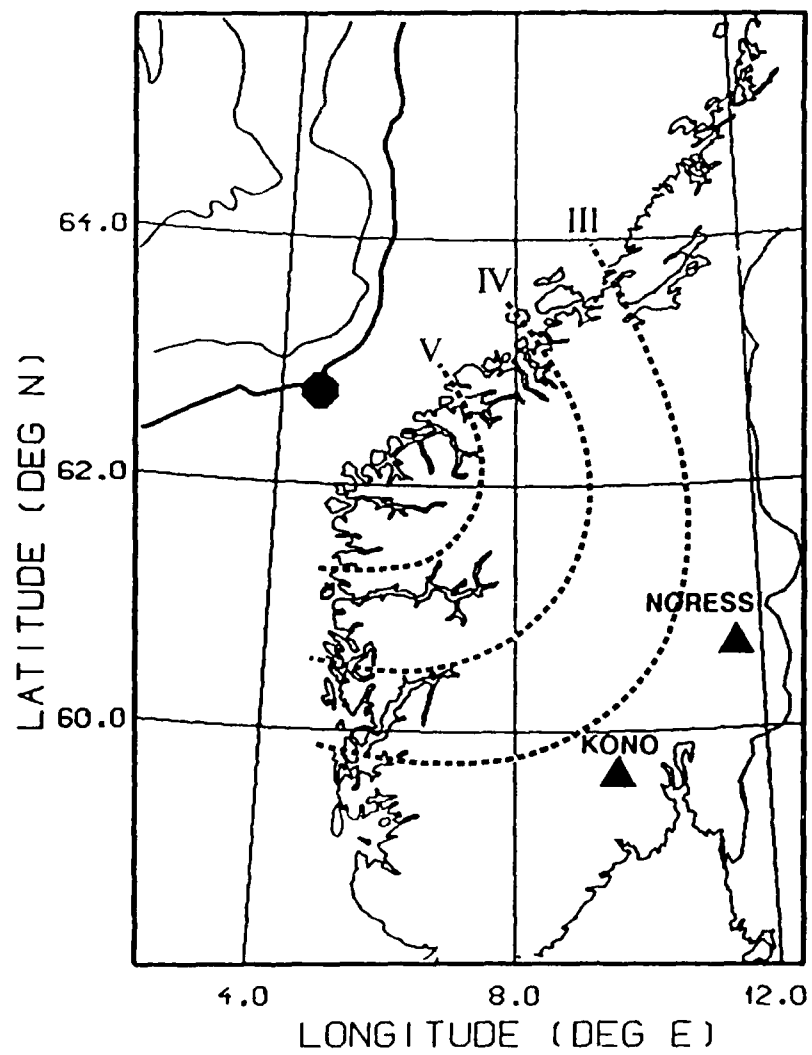


Figure 3

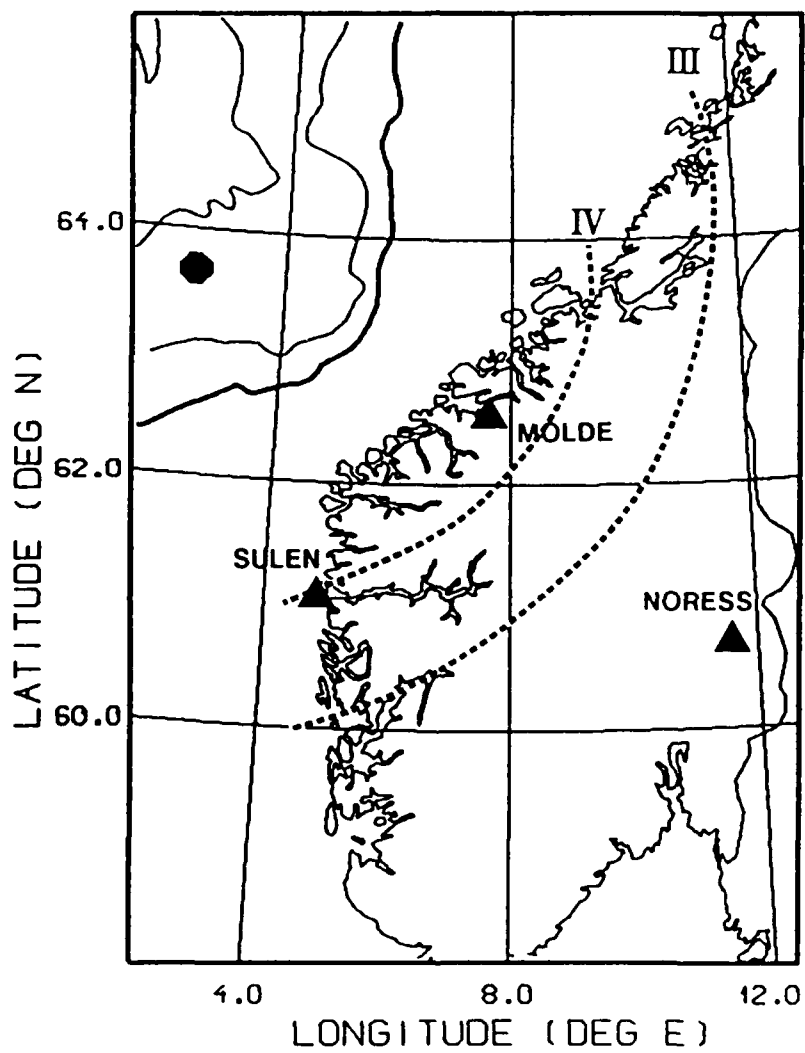


Figure 4

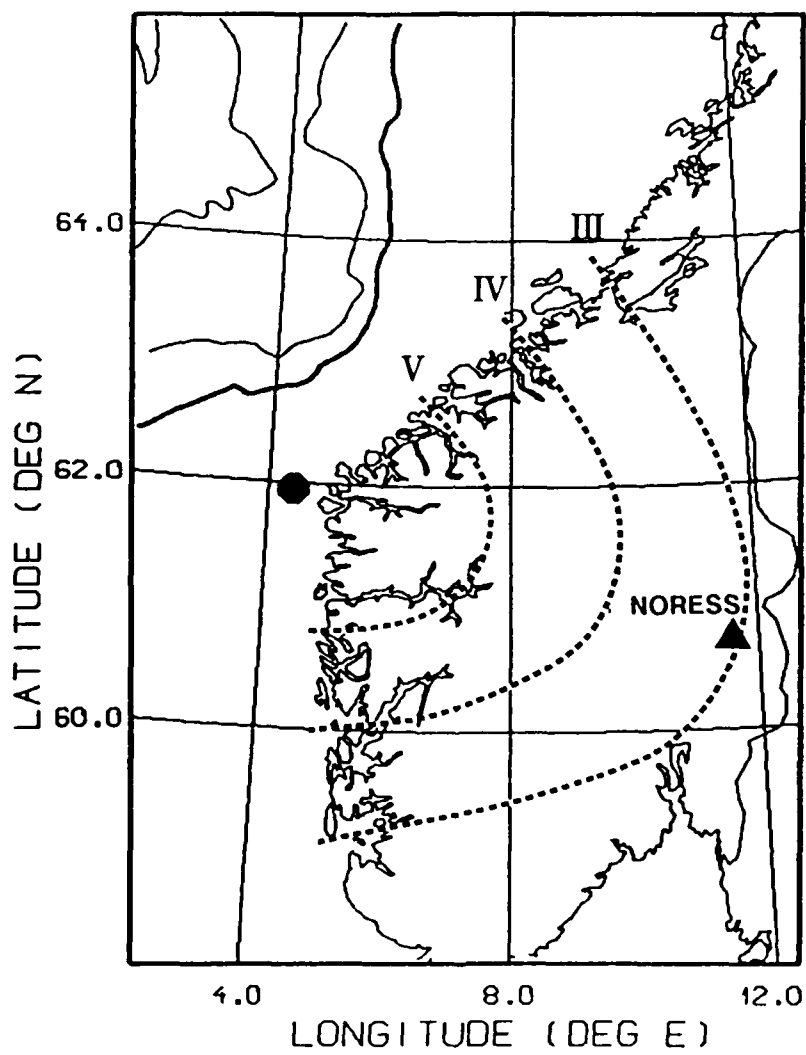


Figure 5

Date: 02 05 86 1754

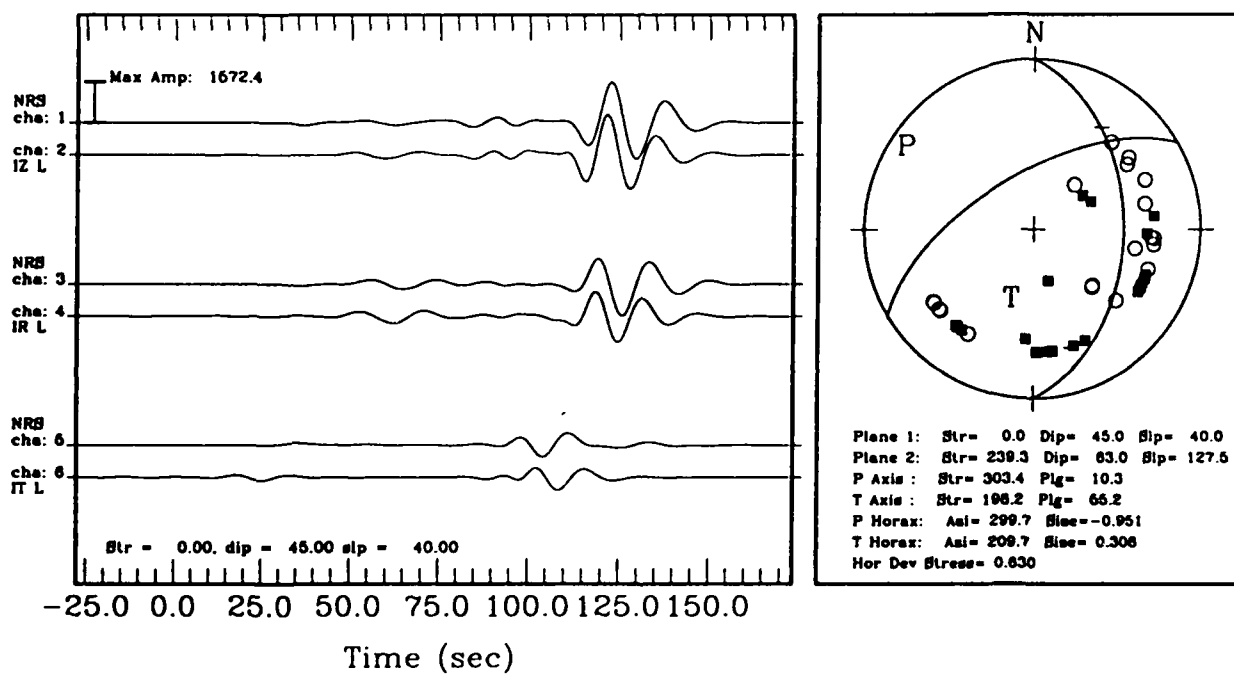


Figure 6

Date: 08 08 88 2000

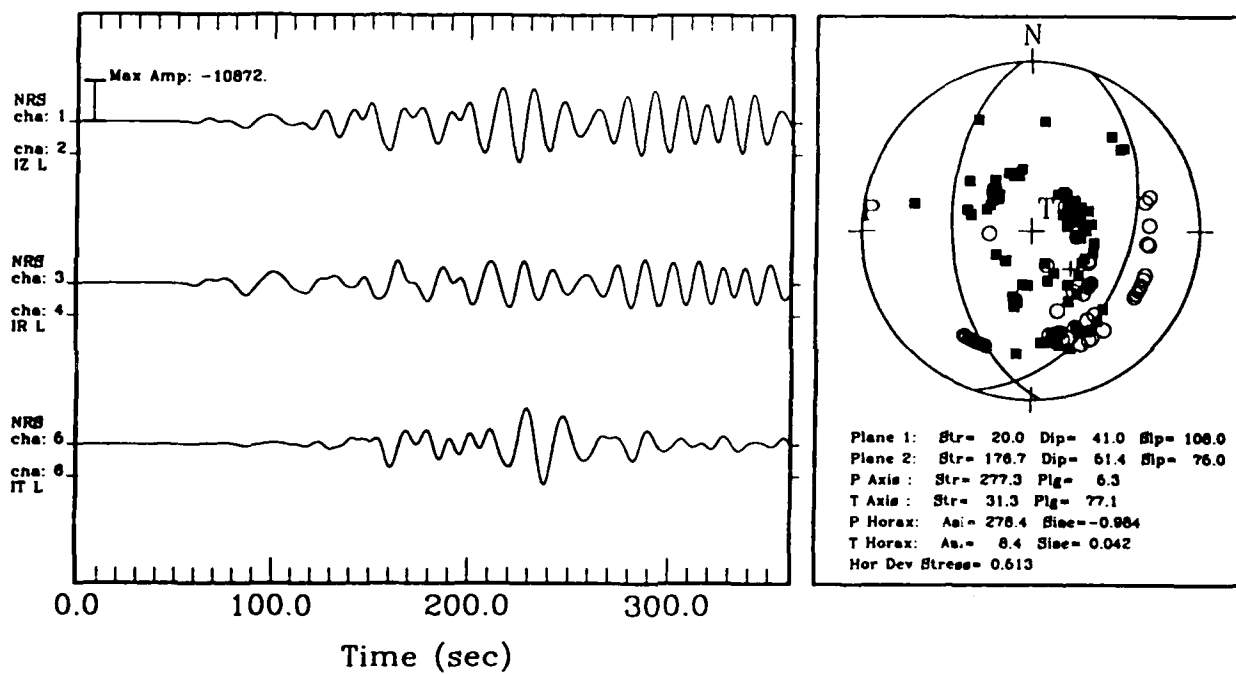


Figure 7

Date: 01 23 89 1407

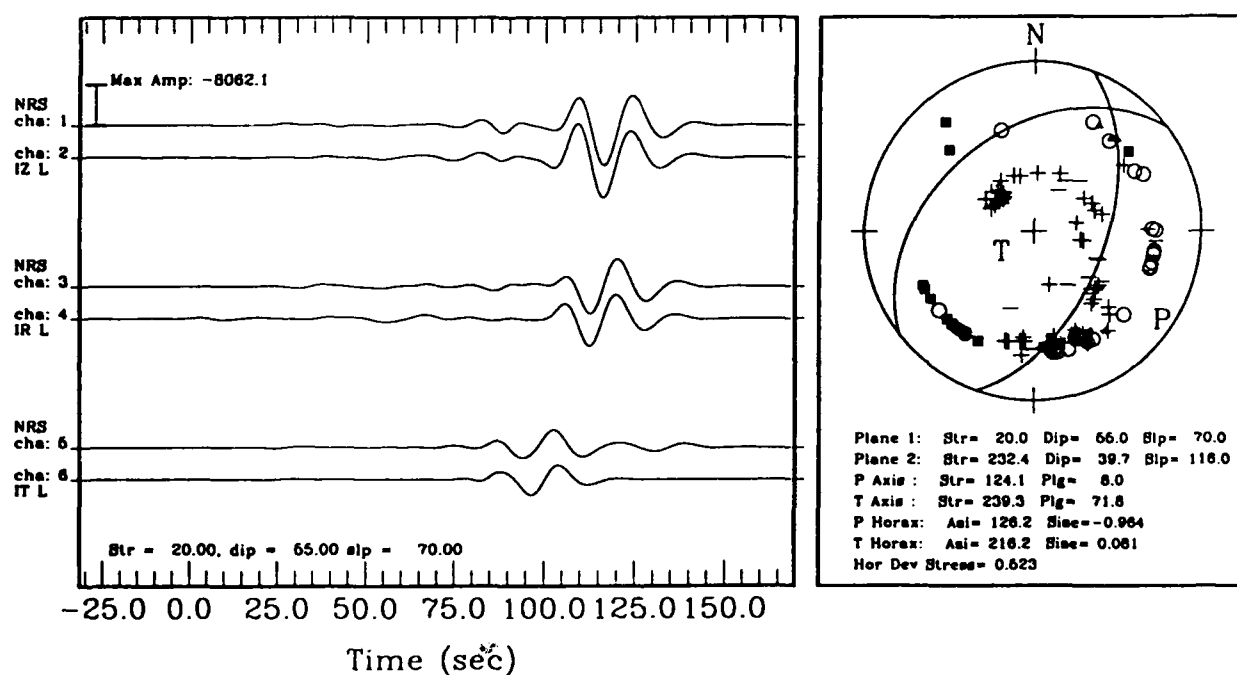


Figure 8

EVENT 1, NORESS 1P, HF

1986 36/17:55:25

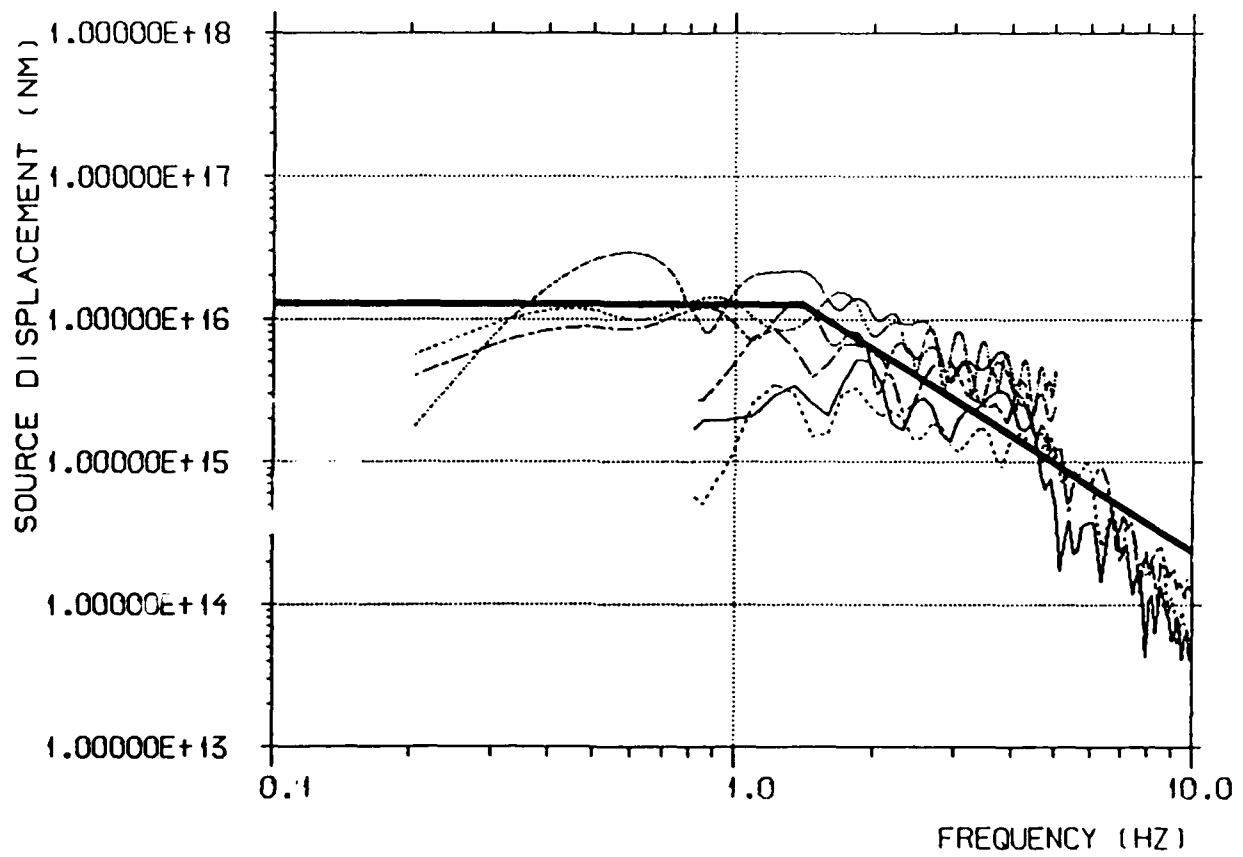


Figure 9

EVENT 2, NORESS IP, MOL, SUE

1988 221/20: 1:49

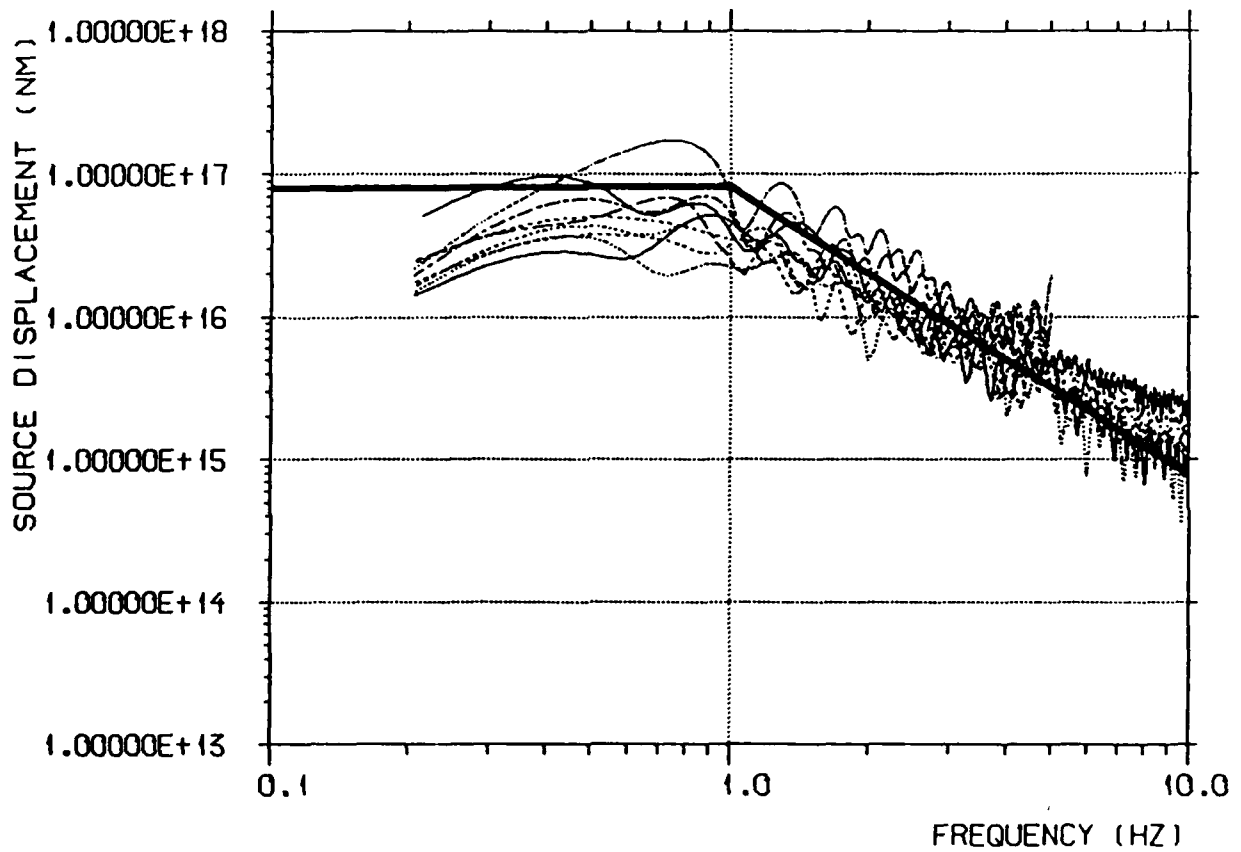


Figure 10

EVENT 3, NORESS IP, HF

1989 23/14: 8:17

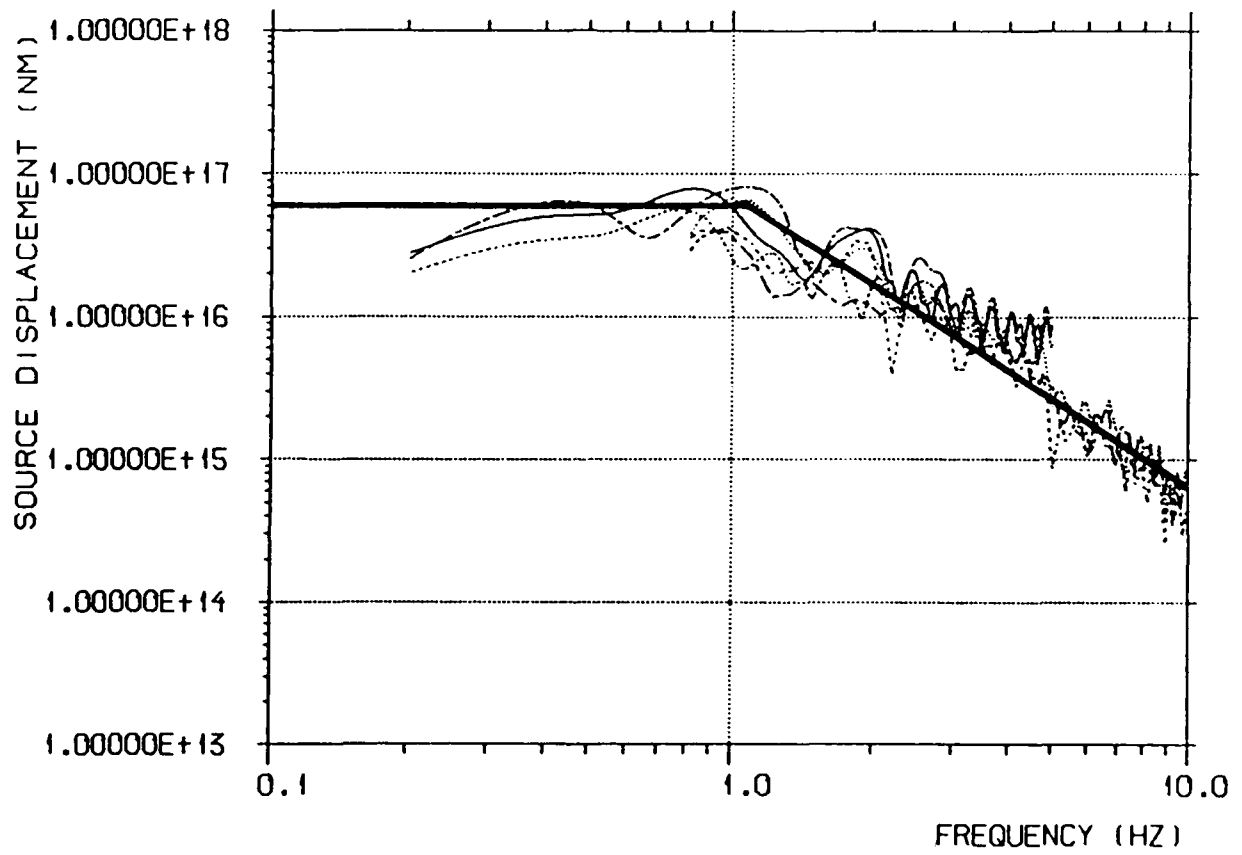


Figure 11

EVENT 2, NORESS, PREDICTIONS

1988 221/20: 1:12

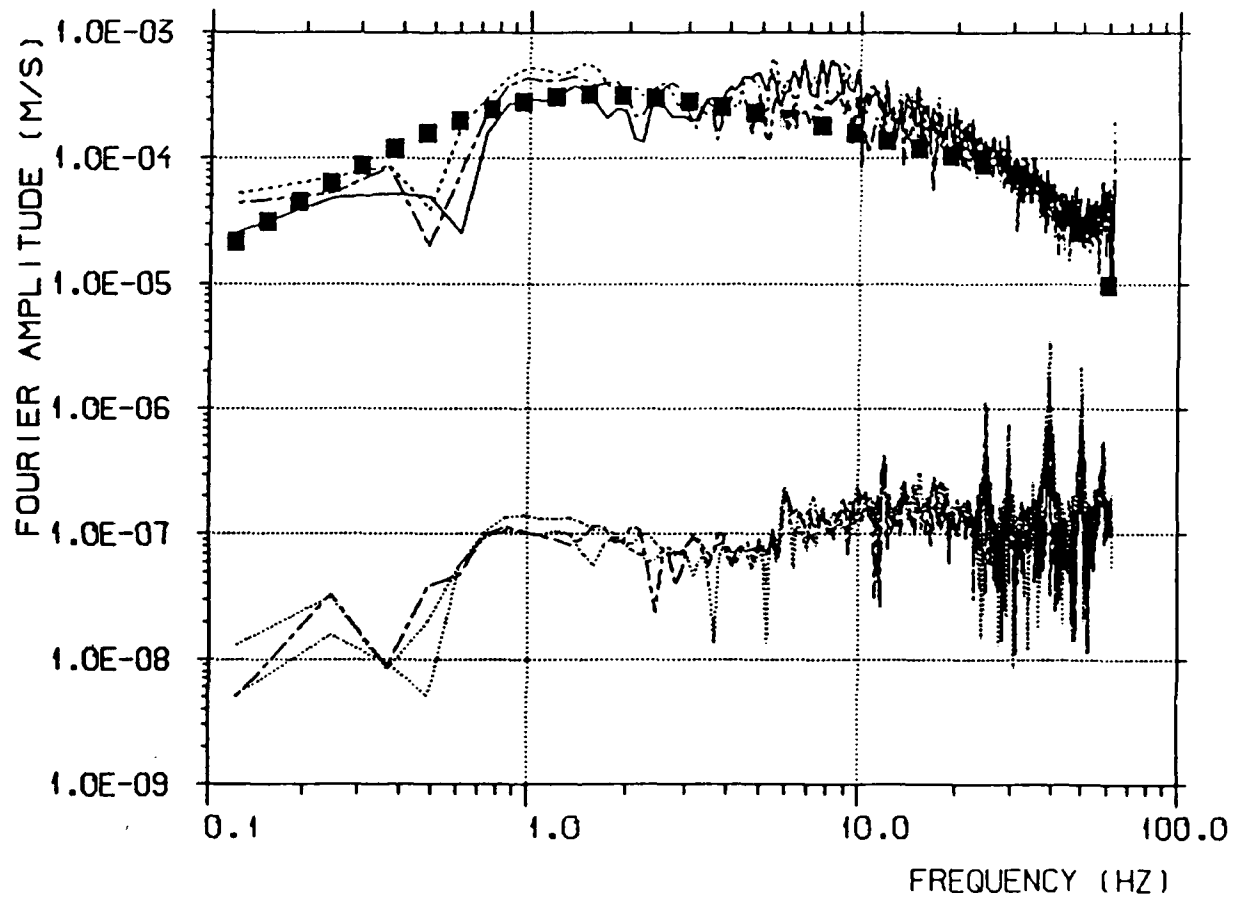


Figure 12

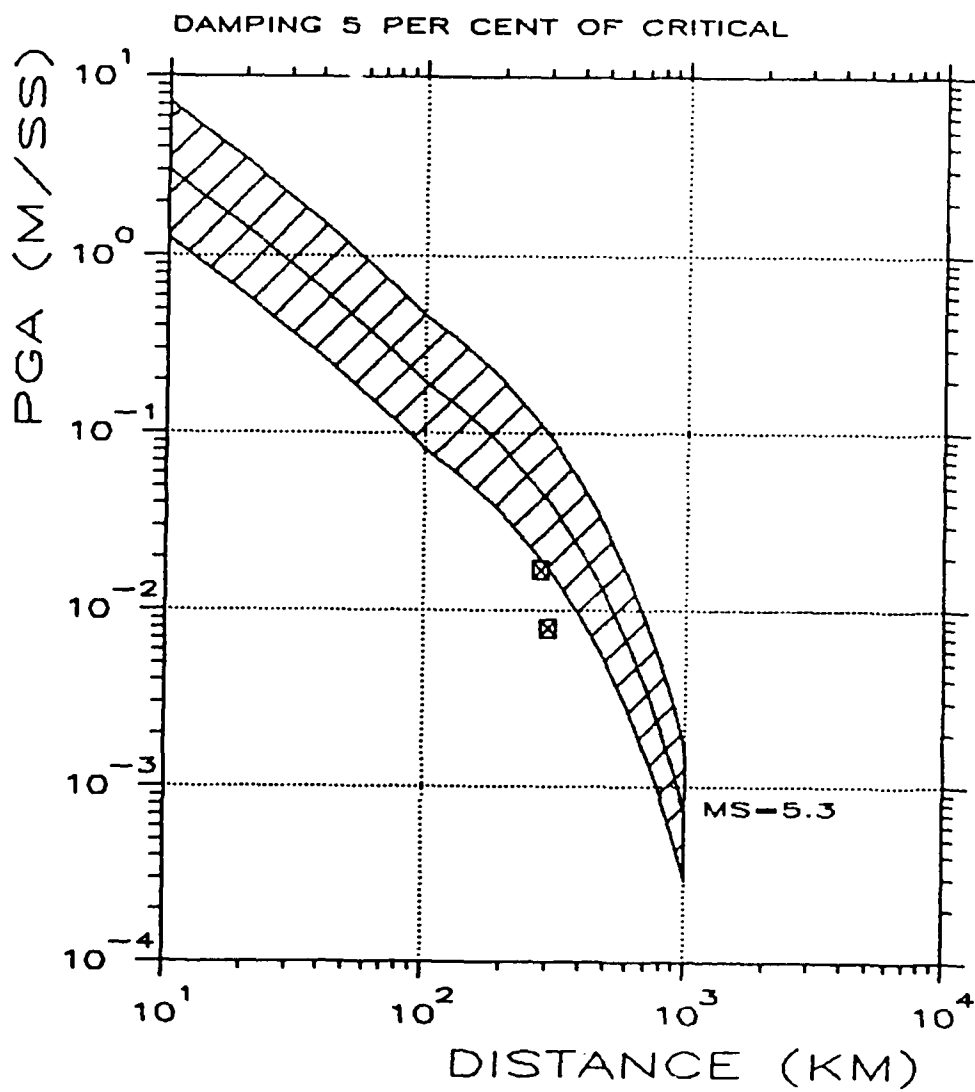


Figure 13

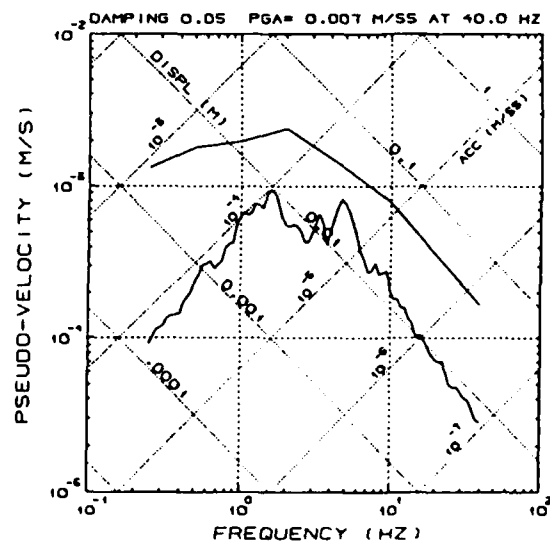
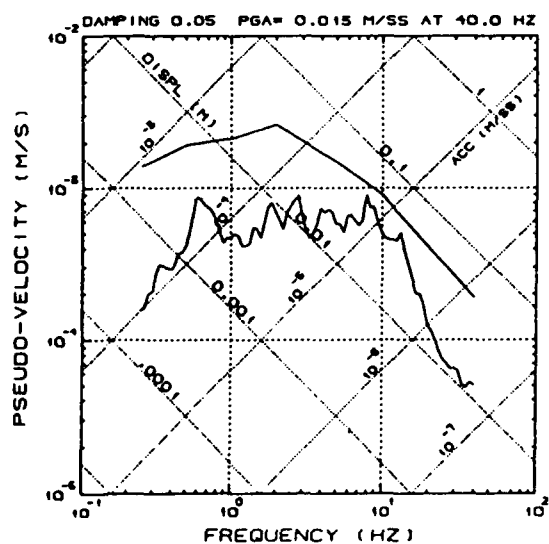
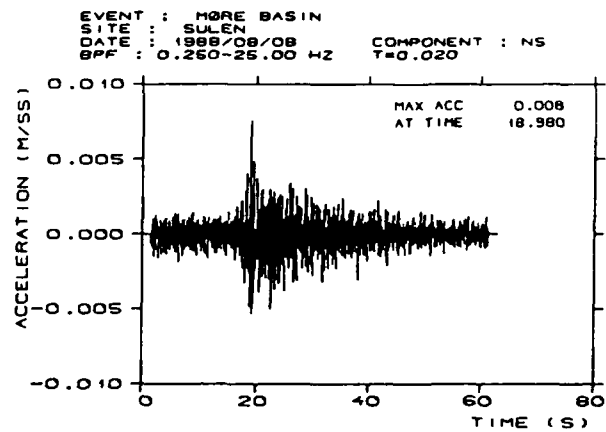
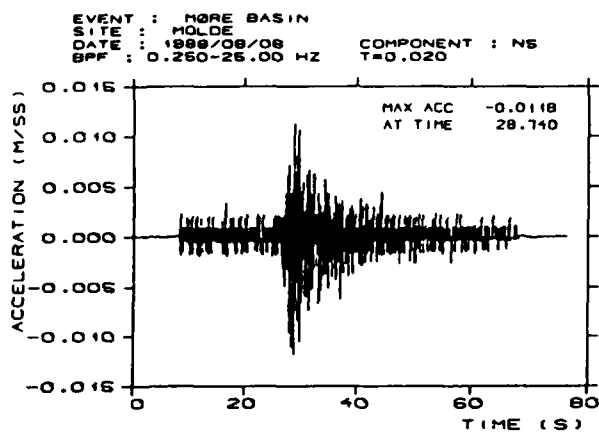


Figure 14

CONTRACTORS (United States)

Prof. Thomas Ahrens
Seismological Lab, 252-21
Division of Geological & Planetary Sciences
California Institute of Technology
Pasadena, CA 91125

Prof. Charles B. Archambeau
CIRES
University of Colorado
Boulder, CO 80309

Prof. Muawia Barazangi
Institute for the Study of the Continent
Cornell University
Ithaca, NY 14853

Dr. Douglas R. Baumgardt
ENSCO, Inc
5400 Port Royal Road
Springfield, VA 22151-2388

Prof. Jonathan Berger
IGPP, A-025
Scripps Institution of Oceanography
University of California, San Diego
La Jolla, CA 92093

Dr. Lawrence J. Burdick
Woodward-Clyde Consultants
566 El Dorado Street
Pasadena, CA 91109-3245

Dr. Karl Coyner
New England Research, Inc.
76 Olcott Drive
White River Junction, VT 05001

Prof. Vernon F. Cormier
Department of Geology & Geophysics
U-45, Room 207
The University of Connecticut
Storrs, CT 06268

Prof. Steven Day
Department of Geological Sciences
San Diego State University
San Diego, CA 92182

Dr. Zoltan A. Der
ENSCO, Inc.
5400 Port Royal Road
Springfield, VA 22151-2388

Prof. John Ferguson
Center for Lithospheric Studies
The University of Texas at Dallas
P.O. Box 830688
Richardson, TX 75083-0688

Prof. Stanley Flatte
Applied Sciences Building
University of California
Santa Cruz, CA 95064

Dr. Alexander Florence
SRI International
333 Ravenswood Avenue
Menlo Park, CA 94025-3493

Prof. Henry L. Gray
Vice Provost and Dean
Department of Statistical Sciences
Southern Methodist University
Dallas, TX 75275

Dr. Indra Gupta
Teledyne Geotech
314 Montgomery Street
Alexandria, VA 22314

Prof. David G. Harkrider
Seismological Laboratory
Division of Geological & Planetary Sciences
California Institute of Technology
Pasadena, CA 91125

Prof. Donald V. Helmberger
Seismological Laboratory
Division of Geological & Planetary Sciences
California Institute of Technology
Pasadena, CA 91125

Prof. Eugene Herrin
Institute for the Study of Earth and Man
Geophysical Laboratory
Southern Methodist University
Dallas, TX 75275

Prof. Robert B. Herrmann
Department of Earth & Atmospheric Sciences
St. Louis University
St. Louis, MO 63156

Prof. Bryan Isacks
Cornell University
Department of Geological Sciences
SNEE Hall
Ithaca, NY 14850

Dr. Rong-Song Jih
Teledyne Geotech
314 Montgomery Street
Alexandria, VA 22314

Prof. Lane R. Johnson
Seismographic Station
University of California
Berkeley, CA 94720

Prof. Alan Kafka
Department of Geology & Geophysics
Boston College
Chestnut Hill, MA 02167

Prof. Fred K. Lamb
University of Illinois at Urbana-Champaign
Department of Physics
1110 West Green Street
Urbana, IL 61801

Prof. Charles A. Langston
Geosciences Department
403 Deike Building
The Pennsylvania State University
University Park, PA 16802

Prof. Thorne Lay
Department of Geological Sciences
1006 C.C. Little Building
University of Michigan
Ann Arbor, MI 48109-1063

Prof. Arthur Lerner-Lam
Lamont-Doherty Geological Observatory
of Columbia University
Palisades, NY 10964

Dr. Christopher Lynnes
Teledyne Geotech
314 Montgomery Street
Alexandria, VA 22314

Prof. Peter Malin
University of California at Santa Barbara
Institute for Crustal Studies
Santa Barbara, CA 93106

Dr. Randolph Martin, III
New England Research, Inc.
76 Olcott Drive
White River Junction, VT 05001

Dr. Gary McCartor
Mission Research Corporation
735 State Street
P.O. Drawer 719
Santa Barbara, CA 93102 (2 copies)

Prof. Thomas V. McEvilly
Seismographic Station
University of California
Berkeley, CA 94720

Dr. Keith L. McLaughlin
S-CUBED
A Division of Maxwell Laboratory
P.O. Box 1620
La Jolla, CA 92038-1620

Prof. William Menke
Lamont-Doherty Geological Observatory
of Columbia University
Palisades, NY 10964

Stephen Miller
SRI International
333 Ravenswood Avenue
Box AF 116
Menlo Park, CA 94025-3493

Prof. Bernard Minster
IGPP, A-025
Scripps Institute of Oceanography
University of California, San Diego
La Jolla, CA 92093

Prof. Brian J. Mitchell
Department of Earth & Atmospheric Sciences
St. Louis University
St. Louis, MO 63156

Mr. Jack Murphy
S-CUBED, A Division of Maxwell Laboratory
11800 Sunrise Valley Drive
Suite 1212
Reston, VA 22091 (2 copies)

Dr. Bao Nguyen
GL/LWH
Hanscom AFB, MA 01731-5000

Prof. John A. Orcutt
IGPP, A-025
Scripps Institute of Oceanography
University of California, San Diego
La Jolla, CA 92093

Prof. Keith Priestley
University of Nevada
Mackay School of Mines
Reno, NV 89557

Prof. Paul G. Richards
Lamont-Doherty Geological Observatory
of Columbia University
Palisades, NY 10964

Dr. Wilmer Rivers
Teledyne Geotech
314 Montgomery Street
Alexandria, VA 22314

Dr. Alan S. Ryall, Jr.
Center for Seismic Studies
1300 North 17th Street
Suite 1450
Arlington, VA 22209-2308

Prof. Charles G. Sammis
Center for Earth Sciences
University of Southern California
University Park
Los Angeles, CA 90089-0741

Prof. Christopher H. Scholz
Lamont-Doherty Geological Observatory
of Columbia University
Palisades, NY 10964

Prof. David G. Simpson
Lamont-Doherty Geological Observatory
of Columbia University
Palisades, NY 10964

Dr. Jeffrey Stevens
S-CUBED
A Division of Maxwell Laboratory
P.O. Box 1620
La Jolla, CA 92038-1620

Prof. Brian Stump
Institute for the Study of Earth & Man
Geophysical Laboratory
Southern Methodist University
Dallas, TX 75275

Prof. Jeremiah Sullivan
University of Illinois at Urbana-Champaign
Department of Physics
1110 West Green Street
Urbana, IL 61801

Prof. Clifford Thurber
University of Wisconsin-Madison
Department of Geology & Geophysics
1215 West Dayton Street
Madison, WI 53706

Prof. M. Nafi Toksoz
Earth Resources Lab
Massachusetts Institute of Technology
42 Carleton Street
Cambridge, MA 02142

Prof. John E. Vidale
University of California at Santa Cruz
Seismological Laboratory
Santa Cruz, CA 95064

Prof. Terry C. Wallace
Department of Geosciences
Building #77
University of Arizona
Tucson, AZ 85721

Dr. Raymond Willeman
GL/LWH
Hanscom AFB, MA 01731-5000

Dr. Lorraine Wolf
GL/LWH
Hanscom AFB, MA 01731-5000

Prof. Francis T. Wu
Department of Geological Sciences
State University of New York
at Binghamton
Vestal, NY 13901

Dr. Monem Abdel-Gawad
Rockwell International Science Center
1049 Camino Dos Rios
Thousand Oaks, CA 91360

Prof. Keiiti Aki
Center for Earth Sciences
University of Southern California
University Park
Los Angeles, CA 90089-0741

Prof. Shelton S. Alexander
Geosciences Department
403 Deike Building
The Pennsylvania State University
University Park, PA 16802

Dr. Ralph Archuleta
Department of Geological Sciences
University of California at Santa Barbara
Santa Barbara, CA 93102

Dr. Thomas C. Bache, Jr.
Science Applications Int'l Corp.
10210 Campus Point Drive
San Diego, CA 92121 (2 copies)

J. Barker
Department of Geological Sciences
State University of New York
at Binghamton
Vestal, NY 13901

Dr. T.J. Bennett
S-CUBED
A Division of Maxwell Laboratory
11800 Sunrise Valley Drive, Suite 1212
Reston, VA 22091

Mr. William J. Best
907 Westwood Drive
Vienna, VA 22180

Dr. N. Biswas
Geophysical Institute
University of Alaska
Fairbanks, AK 99701

Dr. G.A. Bollinger
Department of Geological Sciences
Virginia Polytechnical Institute
21044 Derring Hall
Blacksburg, VA 24061

Dr. Stephen Bratt
Science Applications Int'l Corp.
10210 Campus Point Drive
San Diego, CA 92121

Michael Browne
Teledyne Geotech
3401 Shiloh Road
Garland, TX 75041

Mr. Roy Burger
1221 Serry Road
Schenectady, NY 12309

Dr. Robert Burrige
Schlumberger-Doll Research Center
Old Quarry Road
Ridgefield, CT 06877

Dr. Jerry Carter
Rondout Associates
P.O. Box 224
Stone Ridge, NY 12484

Dr. W. Winston Chan
Teledyne Geotech
314 Montgomery Street
Alexandria, VA 22314-1581

Dr. Theodore Cherry
Science Horizons, Inc.
710 Encinitas Blvd., Suite 200
Encinitas, CA 92024 (2 copies)

Prof. Jon F. Claerbout
Department of Geophysics
Stanford University
Stanford, CA 94305

Prof. Robert W. Clayton
Seismological Laboratory
Division of Geological & Planetary Sciences
California Institute of Technology
Pasadena, CA 91125

Prof. F. A. Dahlen
Geological and Geophysical Sciences
Princeton University
Princeton, NJ 08544-0636

Prof. Anton W. Dainty
Earth Resources Lab
Massachusetts Institute of Technology
42 Carleton Street
Cambridge, MA 02142

Prof. Adam Dziewonski
Hoffman Laboratory
Harvard University
20 Oxford St
Cambridge, MA 02138

Prof. John Ebel
Department of Geology & Geophysics
Boston College
Chestnut Hill, MA 02167

Eric Fielding
SNEE Hall
INSTOC
Cornell University
Ithaca, NY 14853

Prof. Donald Forsyth
Department of Geological Sciences
Brown University
Providence, RI 02912

Dr. Anthony Gangi
Texas A&M University
Department of Geophysics
College Station, TX 77843

Dr. Freeman Gilbert
Inst. of Geophysics & Planetary Physics
University of California, San Diego
P.O. Box 109
La Jolla, CA 92037

Mr. Edward Giller
Pacific Sierra Research Corp.
1401 Wilson Boulevard
Arlington, VA 22209

Dr. Jeffrey W. Given
Sierra Geophysics
11255 Kirkland Way
Kirkland, WA 98033

Prof. Steven Grand
University of Texas at Austin
Department of Geological Sciences
Austin, TX 78713-7909

Prof. Roy Greenfield
Geosciences Department
403 Deike Building
The Pennsylvania State University
University Park, PA 16802

Dan N. Hagedorn
Battelle
Pacific Northwest Laboratories
Battelle Boulevard
Richland, WA 99352

Kevin Hutchenson
Department of Earth Sciences
St. Louis University
3507 Laclede
St. Louis, MO 63103

Prof. Thomas H. Jordan
Department of Earth, Atmospheric
and Planetary Sciences
Massachusetts Institute of Technology
Cambridge, MA 02139

Robert C. Kemerait
ENSCO, Inc.
445 Pineda Court
Melbourne, FL 32940

William Kikendall
Teledyne Geotech
3401 Shiloh Road
Garland, TX 75041

Prof. Leon Knopoff
University of California
Institute of Geophysics & Planetary Physics
Los Angeles, CA 90024

Prof. L. Timothy Long
School of Geophysical Sciences
Georgia Institute of Technology
Atlanta, GA 30332

Dr. George Mellman
Sierra Geophysics
11255 Kirkland Way
Kirkland, WA 98033

Prof. John Nabelek
College of Oceanography
Oregon State University
Corvallis, OR 97331

Prof. Geza Nagy
University of California, San Diego
Department of Ames, M.S. B-010
La Jolla, CA 92093

Prof. Amos Nur
Department of Geophysics
Stanford University
Stanford, CA 94305

Prof. Jack Oliver
Department of Geology
Cornell University
Ithaca, NY 14850

Prof. Robert Phinney
Geological & Geophysical Sciences
Princeton University
Princeton, NJ 08544-0636

Dr. Paul Pomeroy
Rondout Associates
P.O. Box 224
Stone Ridge, NY 12484

Dr. Jay Pulli
RADIX System, Inc.
2 Taft Court, Suite 203
Rockville, MD 20850

Dr. Norton Rimer
S-CUBED
A Division of Maxwell Laboratory
P.O. Box 1620
La Jolla, CA 92038-1620

Prof. Larry J. Ruff
Department of Geological Sciences
1006 C.C. Little Building
University of Michigan
Ann Arbor, MI 48109-1063

Dr. Richard Sailor
TASC Inc.
55 Walkers Brook Drive
Reading, MA 01867

Thomas J. Sereno, Jr.
Science Application Int'l Corp.
10210 Campus Point Drive
San Diego, CA 92121

John Sherwin
Teledyne Geotech
3401 Shiloh Road
Garland, TX 75041

Prof. Robert Smith
Department of Geophysics
University of Utah
1400 East 2nd South
Salt Lake City, UT 84112

Prof. S. W. Smith
Geophysics Program
University of Washington
Seattle, WA 98195

Dr. Stewart Smith
IRIS Inc.
1616 North Fort Myer Drive
Suite 1440
Arlington, VA 22209

Dr. George Sutton
Rondout Associates
P.O. Box 224
Stone Ridge, NY 12484

Prof. L. Sykes
Lamont-Doherty Geological Observatory
of Columbia University
Palisades, NY 10964

Prof. Pradeep Talwani
Department of Geological Sciences
University of South Carolina
Columbia, SC 29208

Prof. Ta-liang Teng
Center for Earth Sciences
University of Southern California
University Park
Los Angeles, CA 90089-0741

Dr. R.B. Tittmann
Rockwell International Science Center
1049 Camino Dos Rios
P.O. Box 1085
Thousand Oaks, CA 91360

Dr. Gregory van der Vink
IRIS, Inc.
1616 North Fort Myer Drive
Suite 1440
Arlington, VA 22209

William R. Walter
Seismological Laboratory
University of Nevada
Reno, NV 89557

•
Dr. Gregory Wojcik
Weidlinger Associates
4410 El Camino Real
Suite 110
Los Altos, CA 94022
,

Prof. John H. Woodhouse
Hoffman Laboratory
Harvard University
20 Oxford Street
Cambridge, MA 02138

Dr. Gregory B. Young
ENSCO, Inc.
5400 Port Royal Road
Springfield, VA 22151-2388

FOREIGN (Others)

Dr. Peter Basham
Earth Physics Branch
Geological Survey of Canada
1 Observatory Crescent
Ottawa, Ontario, CANADA K1A 0Y3

Dr. Eduard Berg
Institute of Geophysics
University of Hawaii
Honolulu, HI 96822

Dr. Michel Bouchon
I.R.I.G.M.-B.P. 68
38402 St. Martin D'Heres
Cedex, FRANCE

Dr. Hilmar Bungum
NTNF/NORSAR
P.O. Box 51
N-2007 Kjeller, NORWAY

Dr. Michel Campillo
Observatoire de Grenoble
I.R.I.G.M.-B.P. 53
38041 Grenoble, FRANCE

Dr. Kin Yip Chun
Geophysics Division
Physics Department
University of Toronto
Ontario, CANADA M5S 1A7

Dr. Alan Douglas
Ministry of Defense
Blacknest, Brimpton
Reading RG7-4RS, UNITED KINGDOM

Dr. Roger Hansen
NTNF/NORSAR
P.O. Box 51
N-2007 Kjeller, NORWAY

Dr. Manfred Henger
Federal Institute for Geosciences & Nat'l Res.
Postfach 510153
D-3000 Hanover 51, FRG

Ms. Eva Johannisson
Senior Research Officer
National Defense Research Inst.
P.O. Box 27322
S-102 54 Stockholm, SWEDEN

Dr. Fekadu Kebede
Seismological Section
Box 12019
S-750 Uppsala, SWEDEN

Dr. Tormod Kvaerna
NTNF/NORSAR
P.O. Box 51
N-2007 Kjeller, NORWAY

Dr. Peter Marshal
Procurement Executive
Ministry of Defense
Blacknest, Brimpton
Reading FG7-4RS, UNITED KINGDOM

Prof. Ari Ben-Menahem
Department of Applied Mathematics
Weizman Institute of Science
Rehovot, ISRAEL 951729

Dr. Robert North
Geophysics Division
Geological Survey of Canada
1 Observatory Crescent
Ottawa, Ontario, CANADA K1A 0Y3

Dr. Frode Ringdal
NTNF/NORSAR
P.O. Box 51
N-2007 Kjeller, NORWAY

Dr. Jorg Schlittenhardt
Federal Institute for Geosciences & Nat'l Res.
Postfach 510153
D-3000 Hannover 51, FEDERAL REPUBLIC OF
GERMANY

Prof. Daniel Walker
University of Hawaii
Institute of Geophysics
Honolulu, HI 96822

FOREIGN CONTRACTORS

Dr. Ramon Cabre, S.J.
Observatorio San Calixto
Casilla 5939
La Paz, Bolivia

• Prof. Hans-Peter Harjes
Institute for Geophysik
Ruhr University/Bochum
P.O. Box 102148
4630 Bochum 1, FRG

• Prof. Eystein Husebye
NTNF/NORSAR
P.O. Box 51
N-2007 Kjeller, NORWAY

Prof. Brian L.N. Kennett
Research School of Earth Sciences
Institute of Advanced Studies
G.P.O. Box 4
Canberra 2601, AUSTRALIA

Dr. Bernard Massinon
Societe Radiomana
27 rue Claude Bernard
75005 Paris, FRANCE (2 Copies)

Dr. Pierre Mecheler
Societe Radiomana
27 rue Claude Bernard
75005 Paris, FRANCE

Dr. Svein Mykkeltveit
NTNF/NORSAR
P.O. Box 51
N-2007 Kjeller, NORWAY

GOVERNMENT

Dr. Ralph Alewine III
DARPA/NMRO
1400 Wilson Boulevard
Arlington, VA 22209-2308

Mr. James C. Battis
GL/LWH
Hanscom AFB, MA 01731-5000

Dr. Robert Blandford
DARPA/NMRO
1400 Wilson Boulevard
Arlington, VA 22209-2308

Eric Chael
Division 9241
Sandia Laboratory
Albuquerque, NM 87185

Dr. John J. Cipar
GL/LWH
Hanscom AFB, MA 01731-5000

Dr. H.B. Durham
Sandia National Laboratory
Albuquerque, NM 87185

Dr. Jack Evernden
USGS - Earthquake Studies
345 Middlefield Road
Menlo Park, CA 94025

Art Frankel
USGS
922 National Center
Reston, VA 22092

Dr. T. Hanks
USGS
Nat'l Earthquake Research Center
345 Middlefield Road
Menlo Park, CA 94025

Dr. James Hannon
Lawrence Livermore Nat'l Laboratory
P.O. Box 808
Livermore, CA 94550

Paul Johnson
ESS-4, Mail Stop J979
Los Alamos National Laboratory
Los Alamos, NM 87545

Janet Johnston
GL/LWH
Hanscom AFB, MA 01731-5000

Dr. Katharine Kadinsky-Cade
GL/LWH
Hanscom AFB, MA 01731-5000

Ms. Ann Kerr
IGPP, A-025
Scripps Institute of Oceanography
University of California, San Diego
La Jolla, CA 92093

Dr. Max Koontz
US Dept of Energy/DP 5
Forrestal Building
1000 Independence Avenue
Washington, DC 20585

Dr. W.H.K. Lee
Office of Earthquakes, Volcanoes,
& Engineering
345 Middlefield Road
Menlo Park, CA 94025

Dr. William Leith
U.S. Geological Survey
Mail Stop 928
Reston, VA 22092

Dr. Richard Lewis
Director, Earthquake Engineering & Geophysics
U.S. Army Corps of Engineers
Box 631
Vicksburg, MS 39180

James F. Lewkowicz
GL/LWH
Hanscom AFB, MA 01731-5000

Mr. Alfred Lieberman
ACDA/VI-OA'State Department Bldg
Room 5726
320 - 21st Street, NW
Washington, DC 20451

Stephen Mangino
GL/LWH
Hanscom AFB, MA 01731-5000

Dr. Frank F. Pilotte
HQ AFTAC/TT
Patrick AFB, FL 32925-6001

Dr. Robert Masse
Box 25046, Mail Stop 967
Denver Federal Center
Denver, CO 80225

Mr. Jack Rachlin
U.S. Geological Survey
Geology, Rm 3 C136
Mail Stop 928 National Center
Reston, VA 22092

Art McGarr
U.S. Geological Survey, MS-977
345 Middlefield Road
Menlo Park, CA 94025

Dr. Robert Reinke
WL/NTESG
Kirtland AFB, NM 87117-6008

Richard Morrow
ACDA/VI, Room 5741
320 21st Street N.W.
Washington, DC 20451

Dr. Byron Ristvet
HQ DNA, Nevada Operations Office
Attn: NVCG
P.O. Box 98539
Las Vegas, NV 89193

Dr. Keith K. Nakanishi
Lawrence Livermore National Laboratory
P.O. Box 808, L-205
Livermore, CA 94550

Dr. George Rothe
HQ AFTAC/TGR
Patrick AFB, FL 32925-6001

Dr. Carl Newton
Los Alamos National Laboratory
P.O. Box 1663
Mail Stop C335, Group ESS-3
Los Alamos, NM 87545

Dr. Michael Shore
Defense Nuclear Agency/SPSS
6801 Telegraph Road
Alexandria, VA 22310

Dr. Kenneth H. Olsen
Los Alamos Scientific Laboratory
P.O. Box 1663
Mail Stop C335, Group ESS-3
Los Alamos, NM 87545

Donald L. Springer
Lawrence Livermore National Laboratory
P.O. Box 808, L-205
Livermore, CA 94550

Howard J. Patton
Lawrence Livermore National Laboratory
P.O. Box 808, L-205
Livermore, CA 94550

Dr. Lawrence Turnbull
OSWR/NED
Central Intelligence Agency
Room 5G48
Washington, DC 20505

Mr. Chris Paine
Office of Senator Kennedy
SR 315
United States Senate
Washington, DC 20510

Dr. Thomas Weaver
Los Alamos National Laboratory
P.O. Box 1663, Mail Stop C335
Los Alamos, NM 87545

Colonel Jerry J. Perrizo
AFOSR/NP, Building 410
Bolling AFB
Washington, DC 20332-6448

J.J. Zucca
Lawrence Livermore National Laboratory
Box 808
Livermore, CA 94550

GL/SULL
Research Library
Hanscom AFB , MA 01731-5000 (2 copies)

Defense Intelligence Agency
Directorate for Scientific &
Technical Intelligence
Washington, DC 20301

Secretary of the Air Force (SAFRD)
Washington, DC 20330

AFTAC/CA
(STINFO)
Patrick AFB, FL 32925-6001

Office of the Secretary Defense
DDR & E
Washington, DC 20330

TACTEC
Battelle Memorial Institute
505 King Avenue
Columbus, OH 43201 (Final Report Only)

HQ DNA
Attn: Technical Library
Washington, DC 20305

DARPA/RMO/RETRIEVAL
1400 Wilson Boulevard
Arlington, VA 22209

DARPA/RMO/Security Office
1400 Wilson Boulevard
Arlington, VA 22209

Geophysics Laboratory
Attn: XO
Hanscom AFB, MA 01731-5000

Geophysics Laboratory
Attn: LW
Hanscom AFB, MA 01731-5000

DARPA/PM
1400 Wilson Boulevard
Arlington, VA 22209

Defense Technical Information Center
Cameron Station
Alexandria, VA 22314 (5 copies)